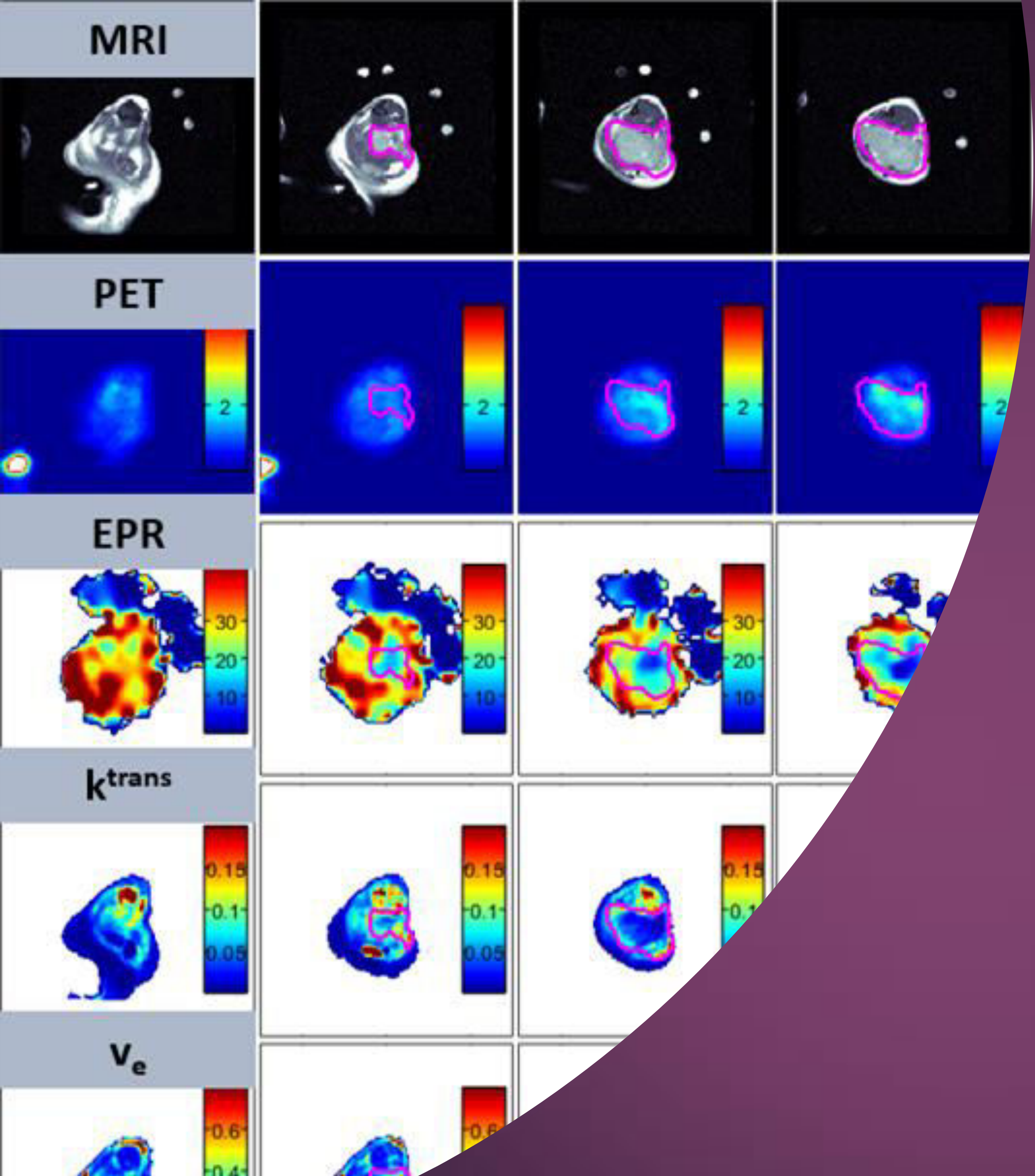

18–25/11/2019
8th SCHOOL
BRNO, Czech Republic
of the European Federation of EPR groups on Advanced EPR

EPR Imaging

Boris Epel

The University of Chicago
Center for EPR Imaging in Vivo Physiology

O2M Technologies, LLC

Disclosure

I am associated with: FeMi Instruments, LLC (SpecMan4EPR software)
O2M Technologies, LLC (EPR preclinical imager)

Outline

- Low Frequency EPR
- Spin Probes
- Oxygen Imaging
- Applications
- Spectral-Spatial Imaging
- Challenges

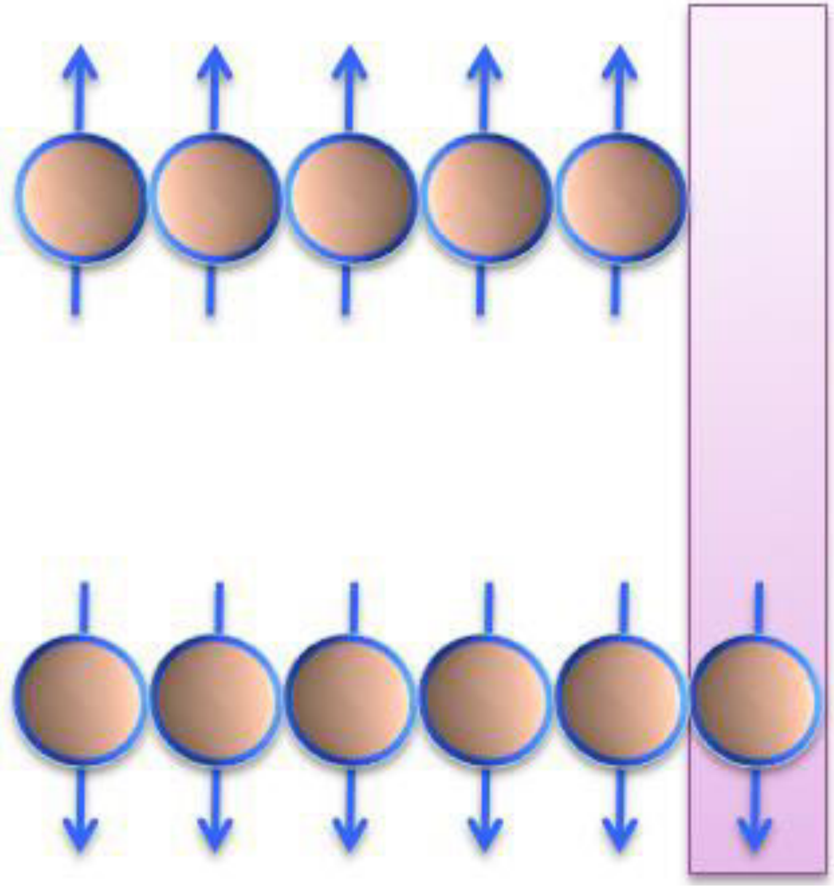

Low Frequency EPR

Electron Paramagnetic Resonance

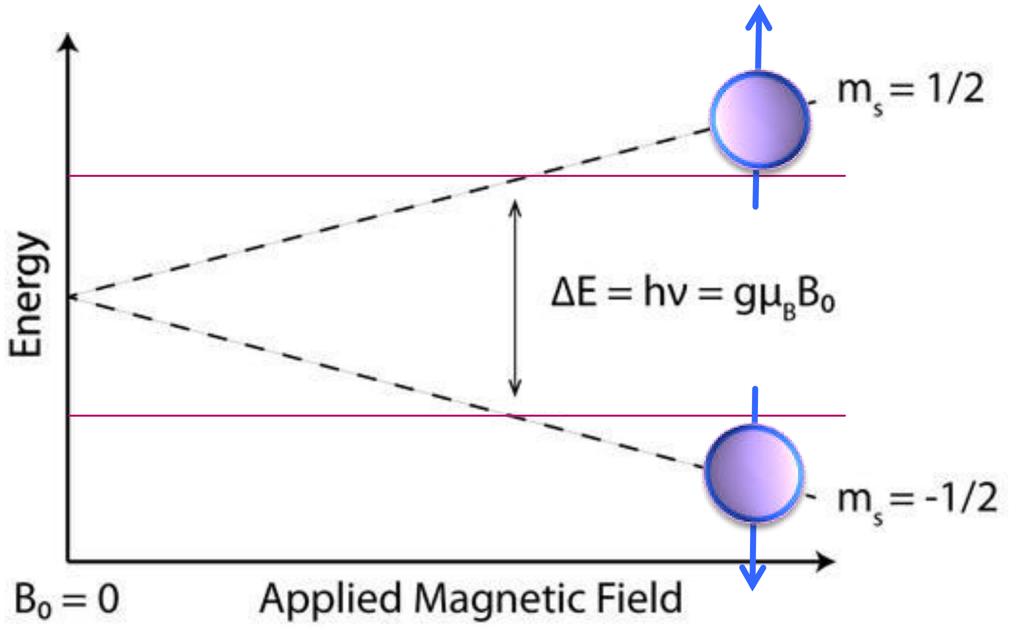

- Zeeman effect - splitting of energy levels into several components in the presence of a static magnetic field
- The transition between these states results in absorption or emission of energy
- The transition can be detected by applying oscillating magnetic field with particular energy (frequency) – magnetic resonance
- <u>Electron magnetic moment is 660 times larger than the proton moment</u>

Experimental approach – continuous wave

- Fix the rf/mw frequency and scan the magnetic field
- (or fix the magnetic field and scan the frequency)

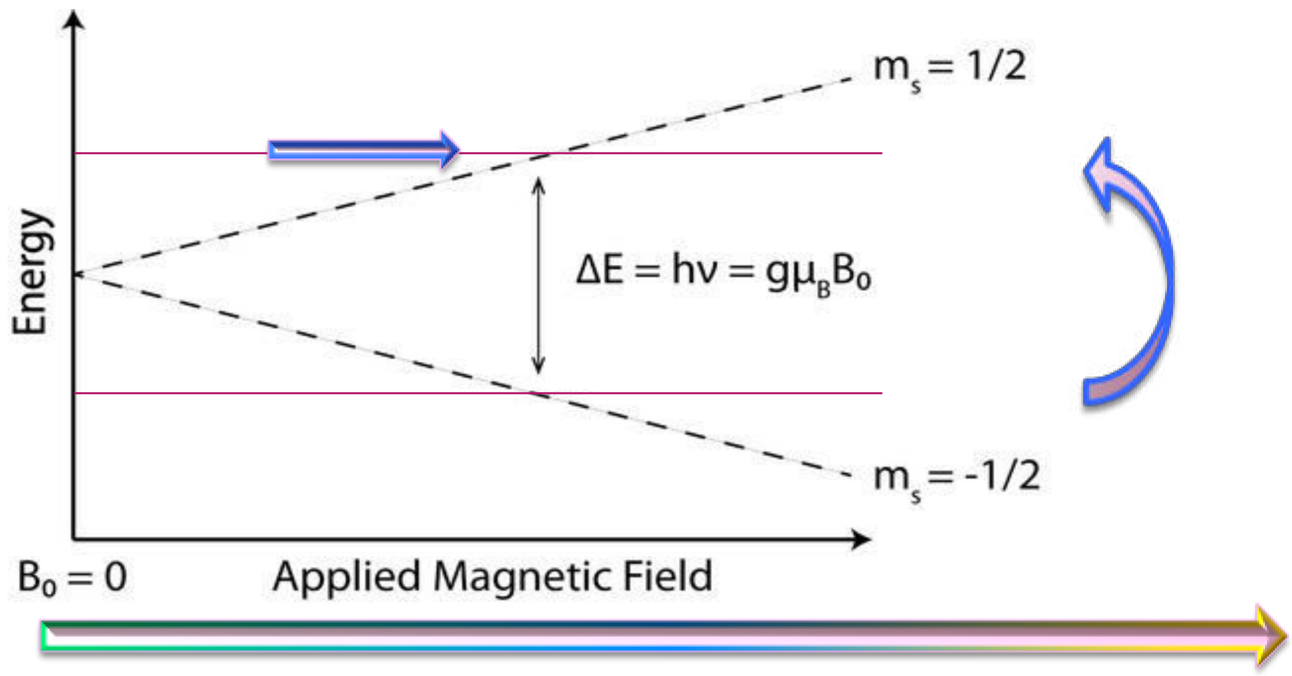

Continuous oscillating rf/mw field at the frequency ν is applied

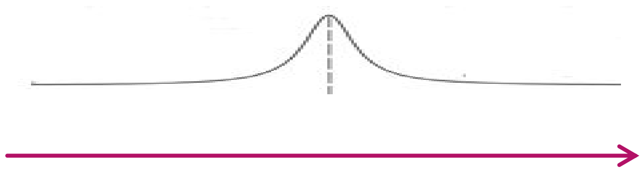

Electron paramagnetic resonance absorption is observed

Experimental approach – pulse EPR

- Magnetic field is fixed, all spins are simultaneously excited using broadband rf pulse
- Fourier transform of the time domain signal gives EPR line shape

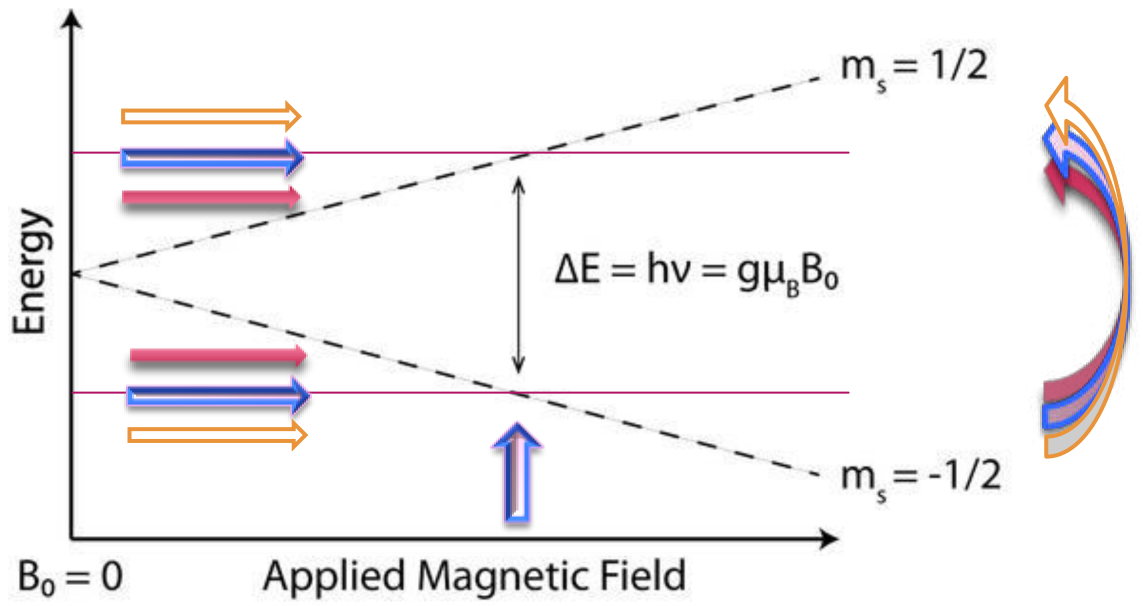

Time trace after rf pulse is observed

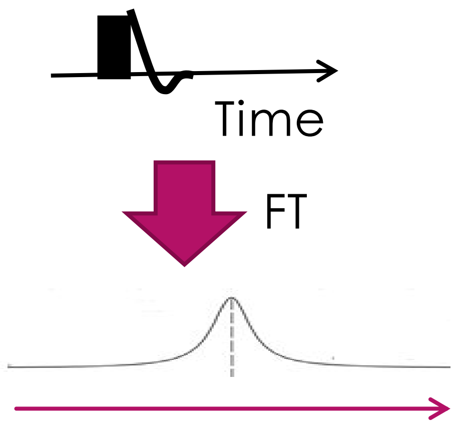

In vivo EPR

- Acquisition at physiologic temperatures
- Objects have fixed size
- Duration of experiment is dictated by animal care regulations
- Instrument design is focused on animal and biomaterials handling
- Resonator Q is dominated by the load (animal)

History of EPR: Dr. E. Zavoyski observed first EPR signals in Kazan University (Russia) in 1944

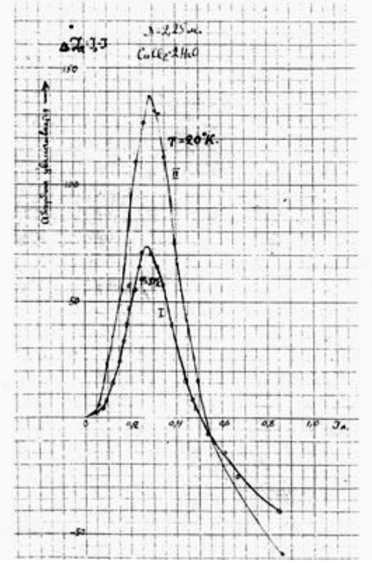

133 MHz
(4.75 mT)
This is the first low field EPR measurement

The choice of frequency

Signal <u>increases with the </u>frequency - Faraday's law + Boltzmann distribution. Noise also increases with frequency but much slower.

Water causes absorption of the RF energy. Eddy currents prevents magnetic field from penetrating deep into the samples. <u>These effects get worse with frequency</u>

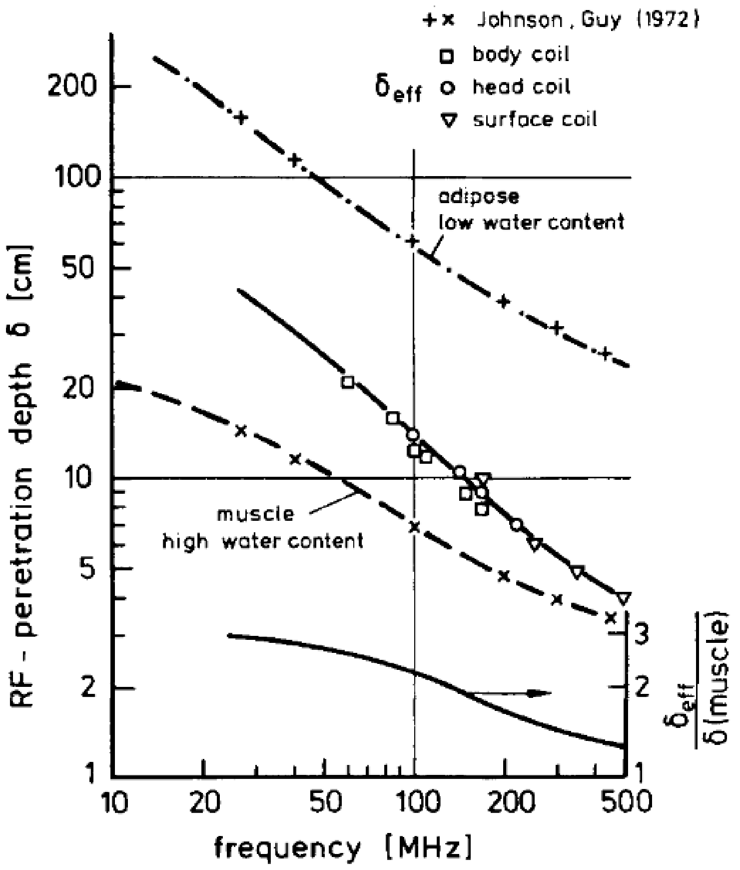

Roschmann, P. (1987). "Radiofrequency Penetration and Absorption in the Human-Body ..." <u>Medical Physics **14**(6): 922-931.</u>

Operational field and frequency

Frequency	~250 MHz	~750 MHz	1-2 GHz
Field	~10mT	~25 mT	
Depth	> 10 cm	6-8 cm	2-3 cm
Object	Rodents, rabbits, (humans)	Mice	Parts of the mouse anatomy

EPR vs ^{1}H MRI

	MRI	EPR
Magnetic field at 250 MHz (our EPR imager frequency)	5.9 T	9 mT
Radiofrequency pulse width	µsec – msec	10 – 100 nsec
Relaxation rates	msec – sec	nsec - µsec
Endogenous probes	Water protons	-
Exogenous probes	-	Nitroxides, trityl
Concentration	>60 M	< 1 mM
Stability	Stable	Minutes
Line width	Hz – kHz	100 kHz - MHz

Magnet and Gradient System

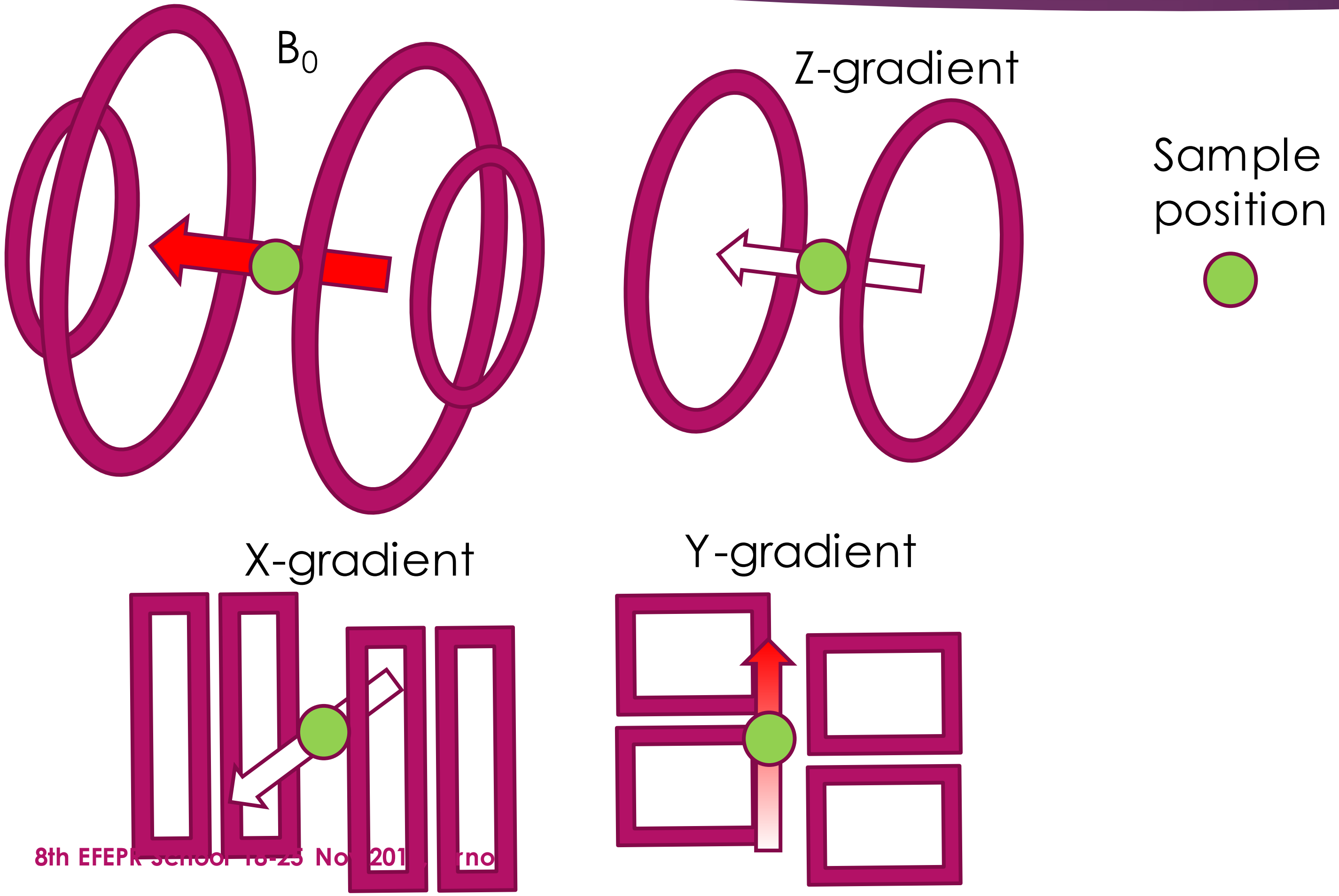

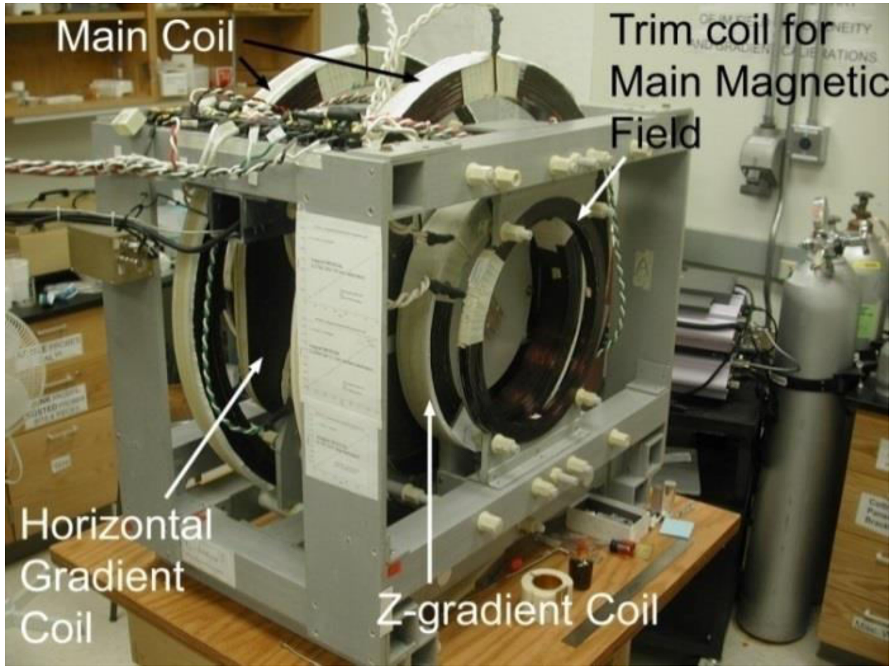

250 MHz / 720 MHz pulse EPR imager

Excitation arm can be substituted with 4GS/s AWG - Arbitrary pulse shapes

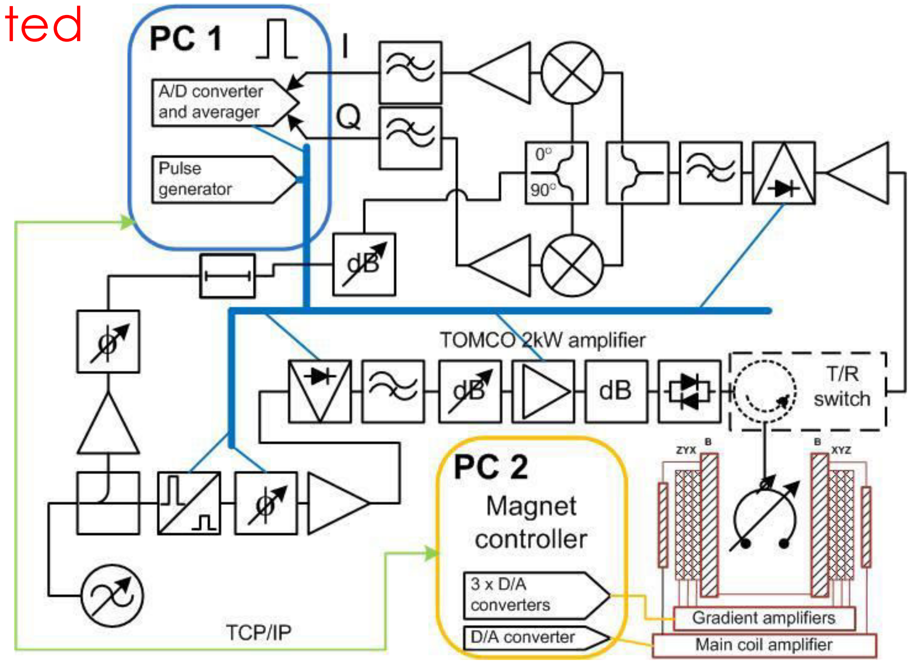

SpecMan4EPR: www.specman4epr.com

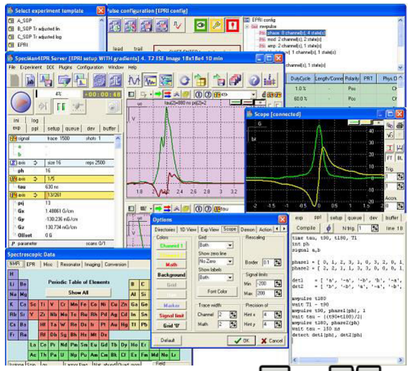

FeMi INSTRUMENTS, LLC

Epel B. *et al.*, Concepts in Magnetic Resonance, 33B (2008) 163-176.
Quine R.W. *et al.*, Concepts in Magnetic Resonance, 15B (2002) 59-91.

Resonators for in vivo Imaging

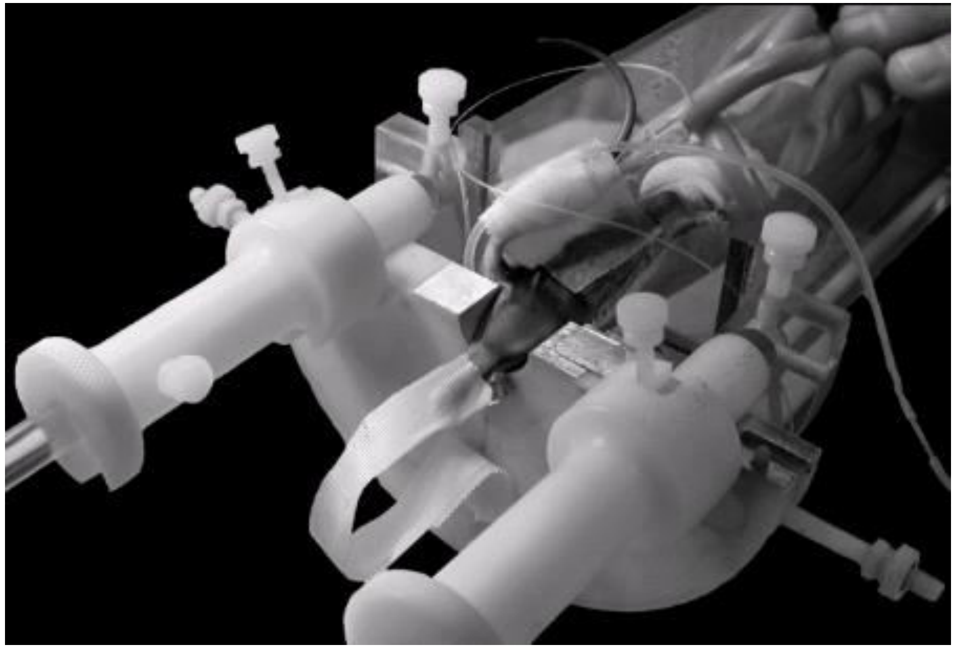

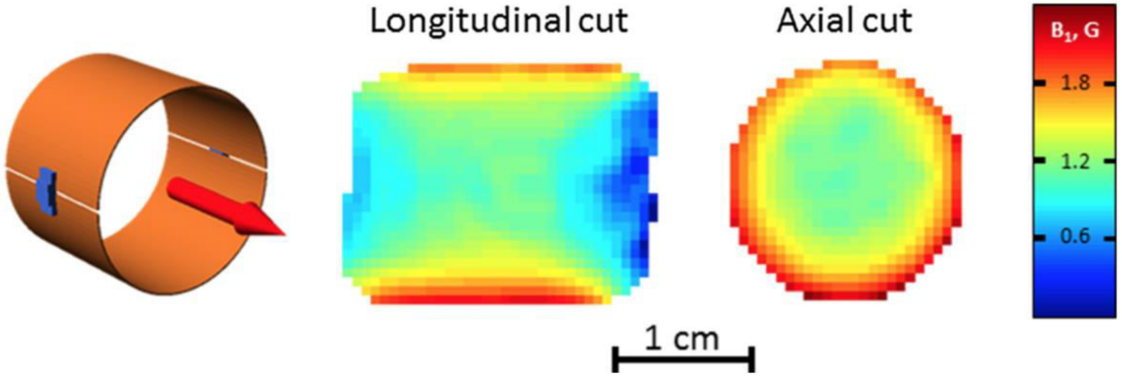

Rinard, G. A., R. W. Quine, L. A. Buchanan, S. S. Eaton, G. R. Eaton, B. Epel, S. V. Sundramoorthy and H. J. Halpern (2017). Applied Magnetic Resonance **48**(11-12): 1227-1247.

In Vivo EPR Oxygen Imaging

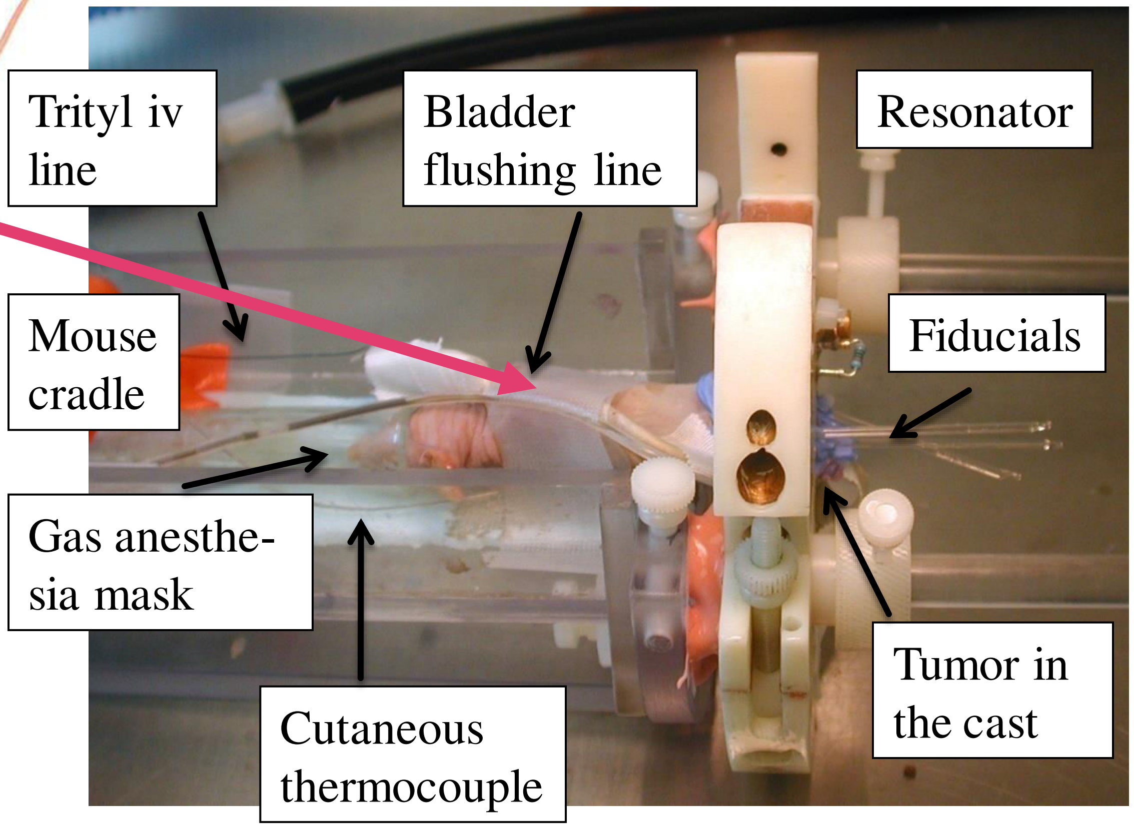

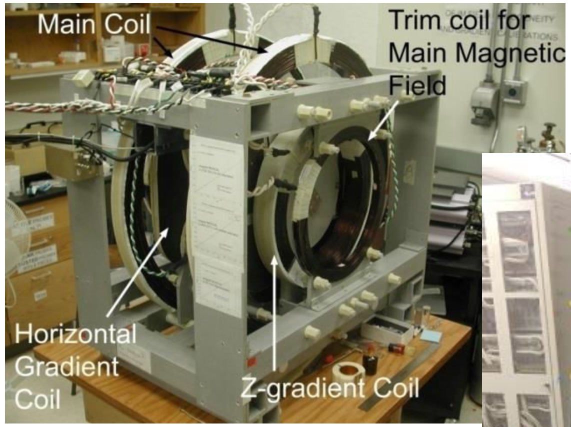

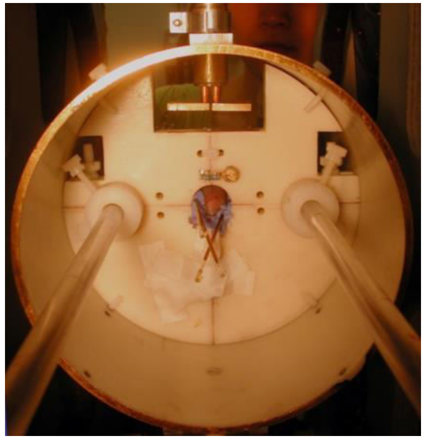

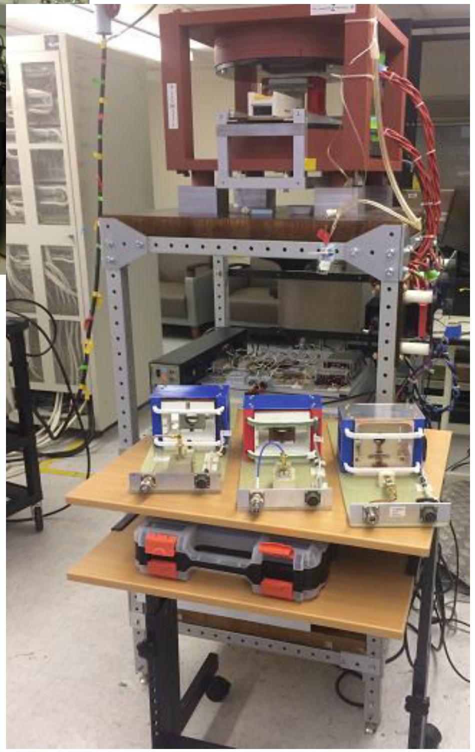

Spin Probes

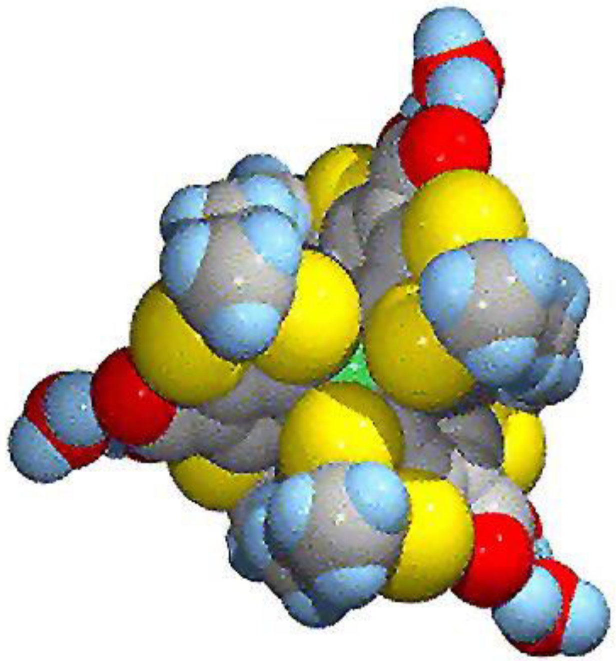

Oxygen Spin Probes

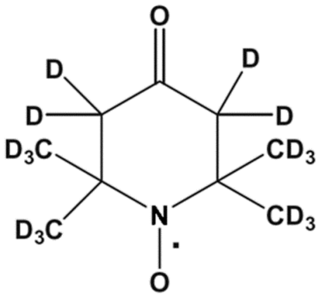

A

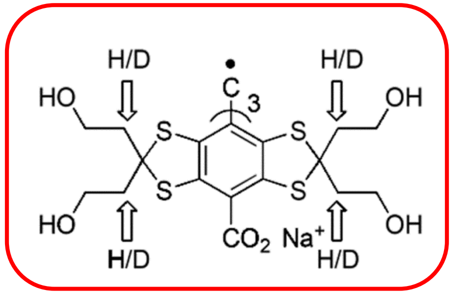

B

C

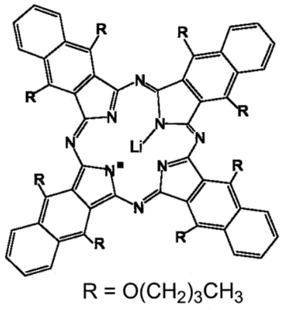

Soluble spin probes

A Nitroxide radicals
B Trityl radicals

- Concentration of oxygen dissolved in a fluid
- Injected systemically / to the tissue of interest

Particulate (insoluble) spin probes

C Lithium phthalocyanine and its derivatives

- Concentration of oxygen in material pores
- Implanted

Molecular oxygen

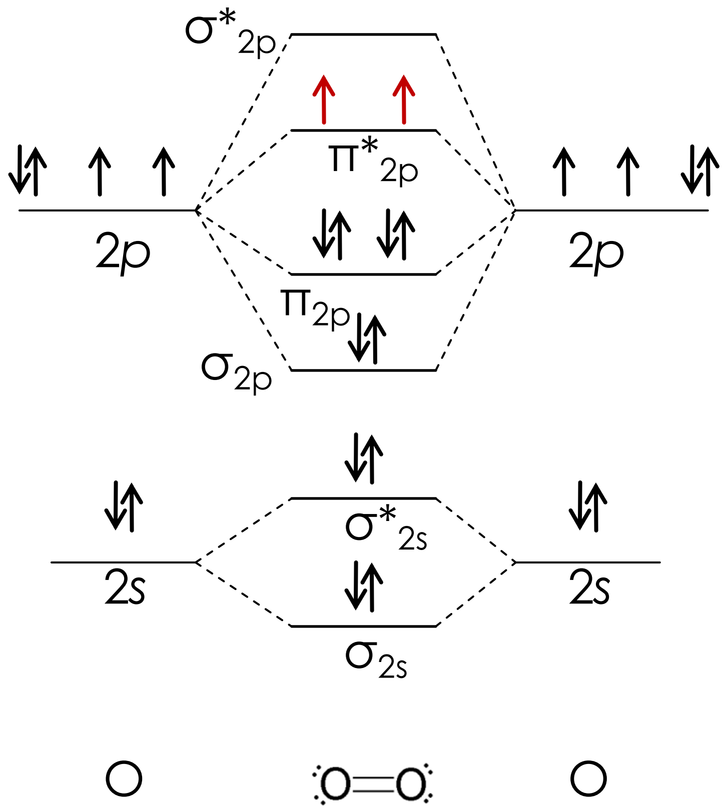

- Two unpaired electrons
- Very fast relaxation time: 1-10 ps
- Can not be observed using room temperature EPR
- Oxygen molecule collides with EPR probe
- Heisenberg exchange – Electron of the spin probe 'feels' the relaxing environment of the oxygen molecule during short time of the collision
- More oxygen – longer the interaction – faster the relaxation

Oxygen Concentration in Solution

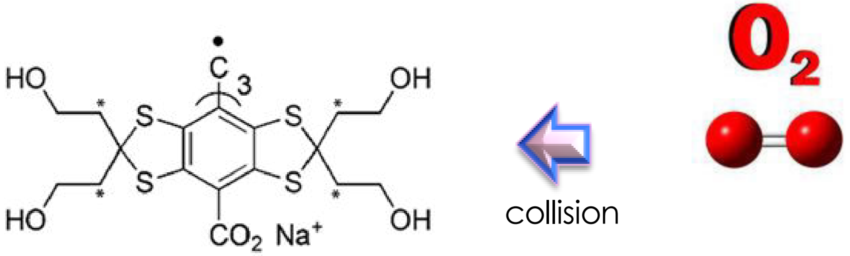

Heisenberg spin exchange

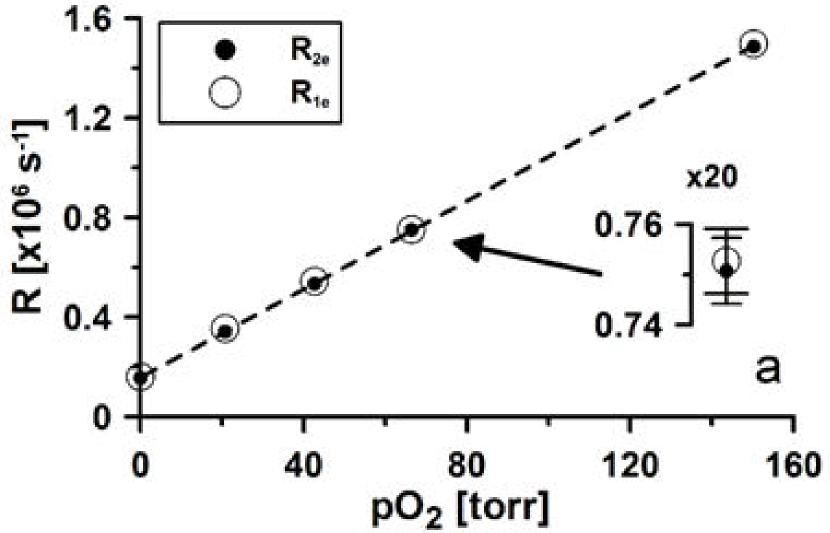

Both spin-spin and spin-lattice relation rates exhibit linear relations with pO_2

Trityls (Spin Probe)

- Synthesized ~1996 by Nicomed Innovations, Sweden, currently GE Healthcare
- Long relaxation: Symmetric shape, fast motion.
  - At physiologic conditions (250MHz) and no O_2 $T_1 \approx T_2 \approx 6 - 7\ \mu s$
  - At 21% O_2 (blood saturated with O_2) $T_1 \approx T_2 \approx 0.6\ \mu s$
  - High sensitivity to O_2 and still measureable using pulse EPR
- Narrow EPR line – high image resolution
- Clearance from a mouse: 5-20 minutes
- Non toxic and biostable
  - Well tolerated by animals
  - The carbon based radical is sterically protected from the environment
- Polar (3+): Does not enter cells. Locates in the extracellular volume.

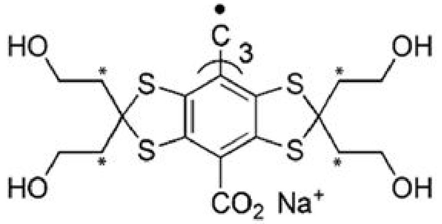

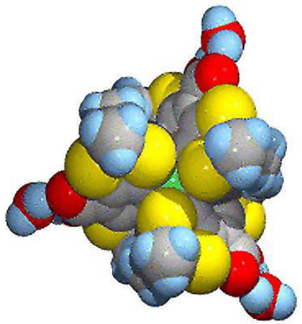

Bowman et al. *J Mag Res* 2004

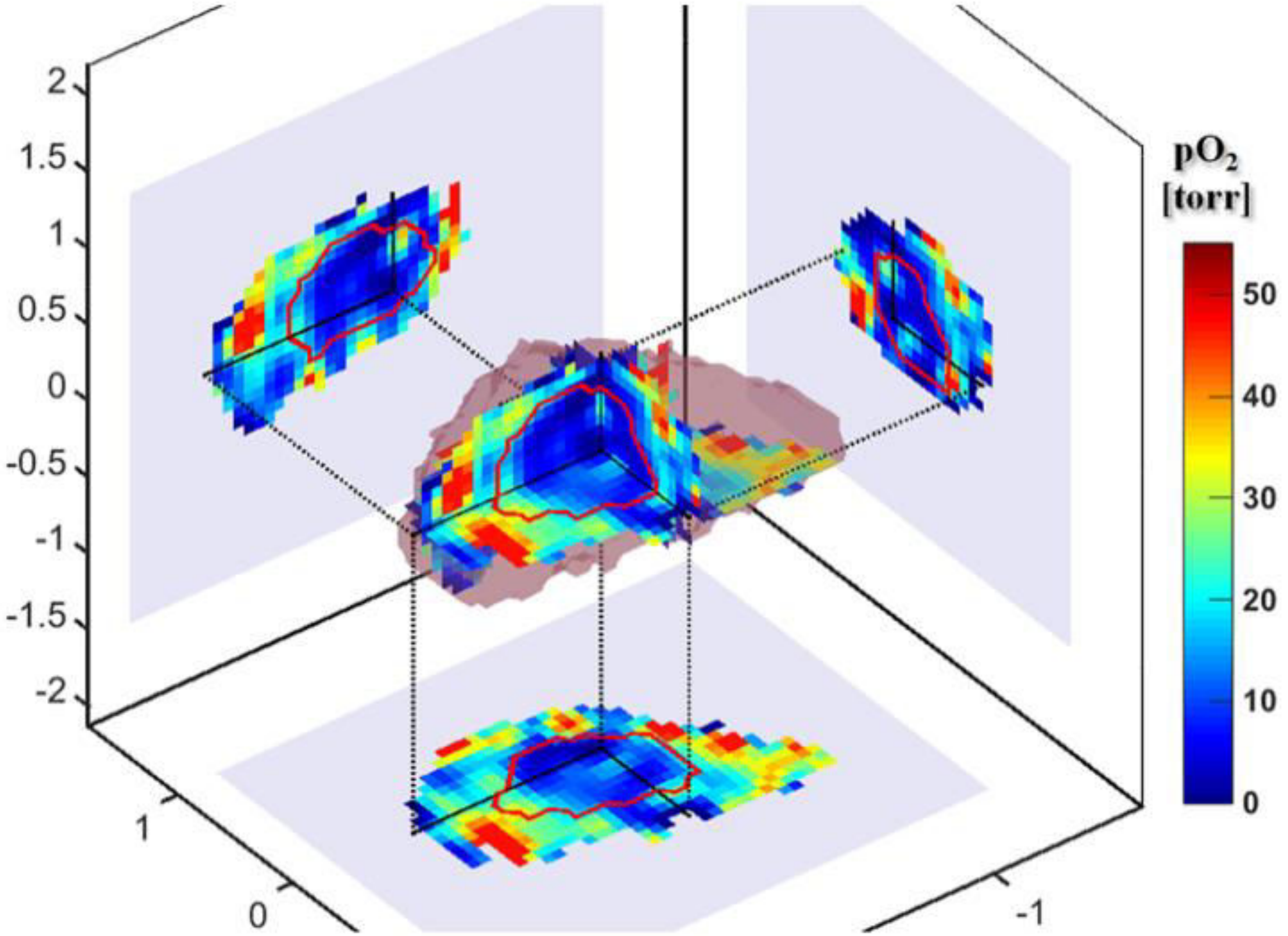

Pulse EPR Oxygen Imaging

Magnetic Resonance Imaging

Prof. Paul Lauterbur (1973)

The position is encoded as a signal frequency using the magnetic field gradients

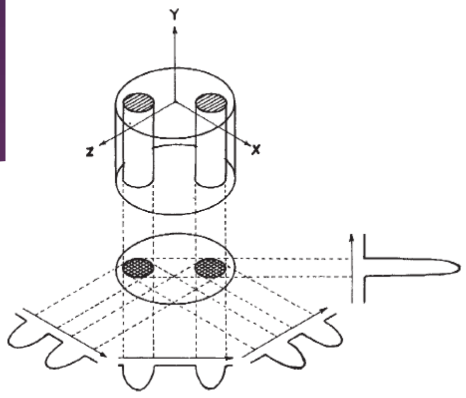

Fig. 1 Relationship between a three-dimensional object, its two-dimensional projection along the Y-axis, and four one-dimensional projections at 45° intervals in the XZ-plane. The arrows indicate the gradient directions.

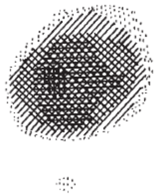

Lauterbur, P. C. (1973). "Image Formation by Induced Local Interactions - Examples Employing Nuclear Magnetic-Resonance." Nature **242**(5394): 190-191.

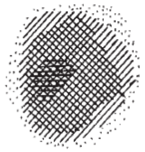

Fig. 2 Proton nuclear magnetic resonance zeugmatogram of the object described in the text, using four relative orientations of object and gradients as diagrammed in Fig. 1.

Modern MRI uses the combination of frequency and phase encoding
EPR Imaging uses Lauterbur's method extended to 3D and 4D

Imaging: Projections

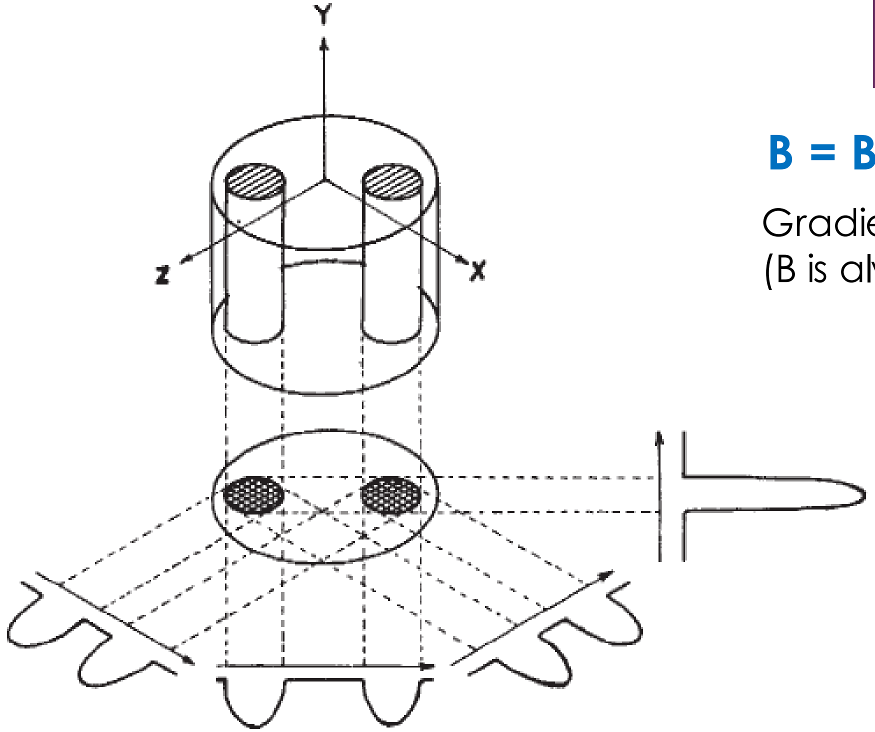

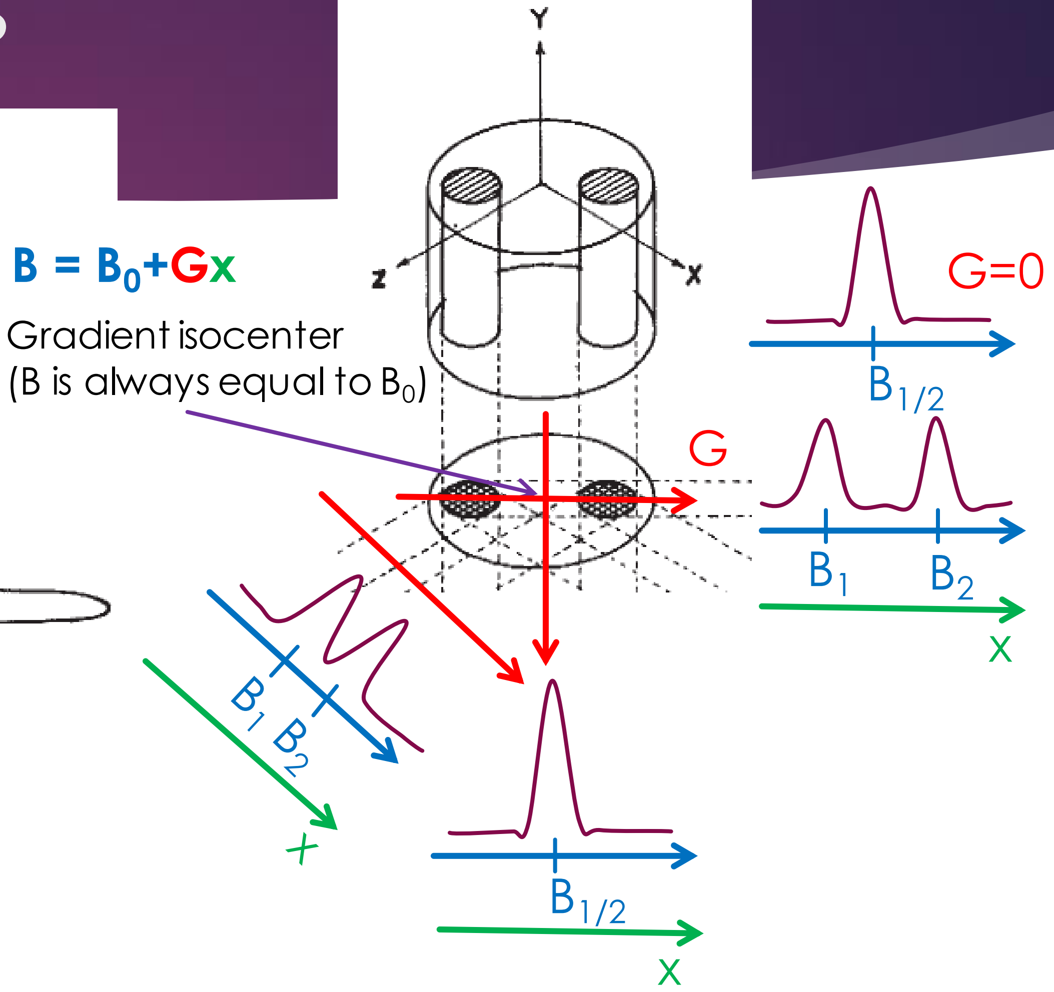

Lauterbur PC. Nature 1973;242(5394):190-191.

Rotation of the gradient direction is mathematically equivalent to rotation of the projection direction in Radon transformation → original object can be restored

Numeric Reconstruction: projection

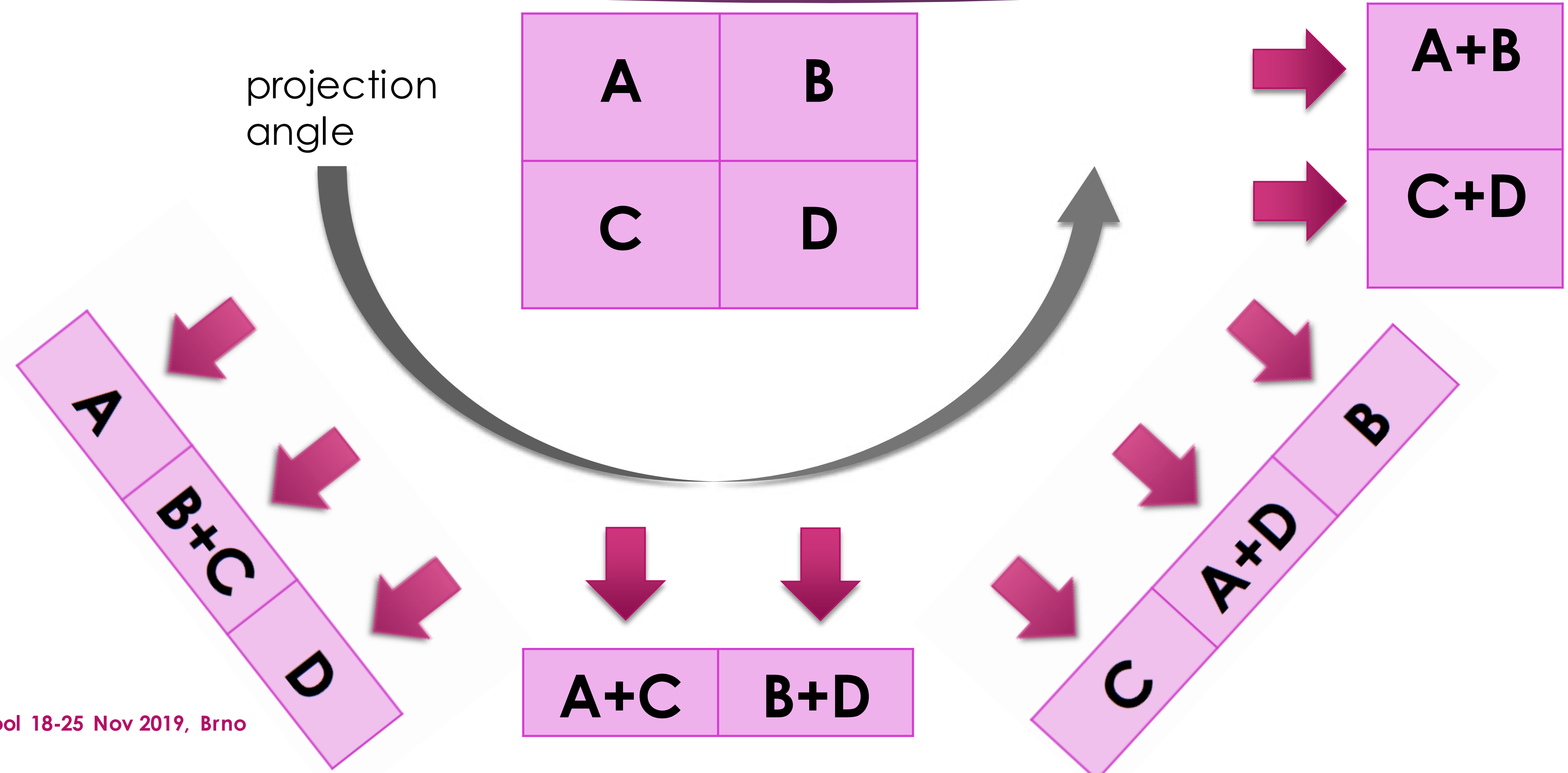

Numeric Reconstruction: problem

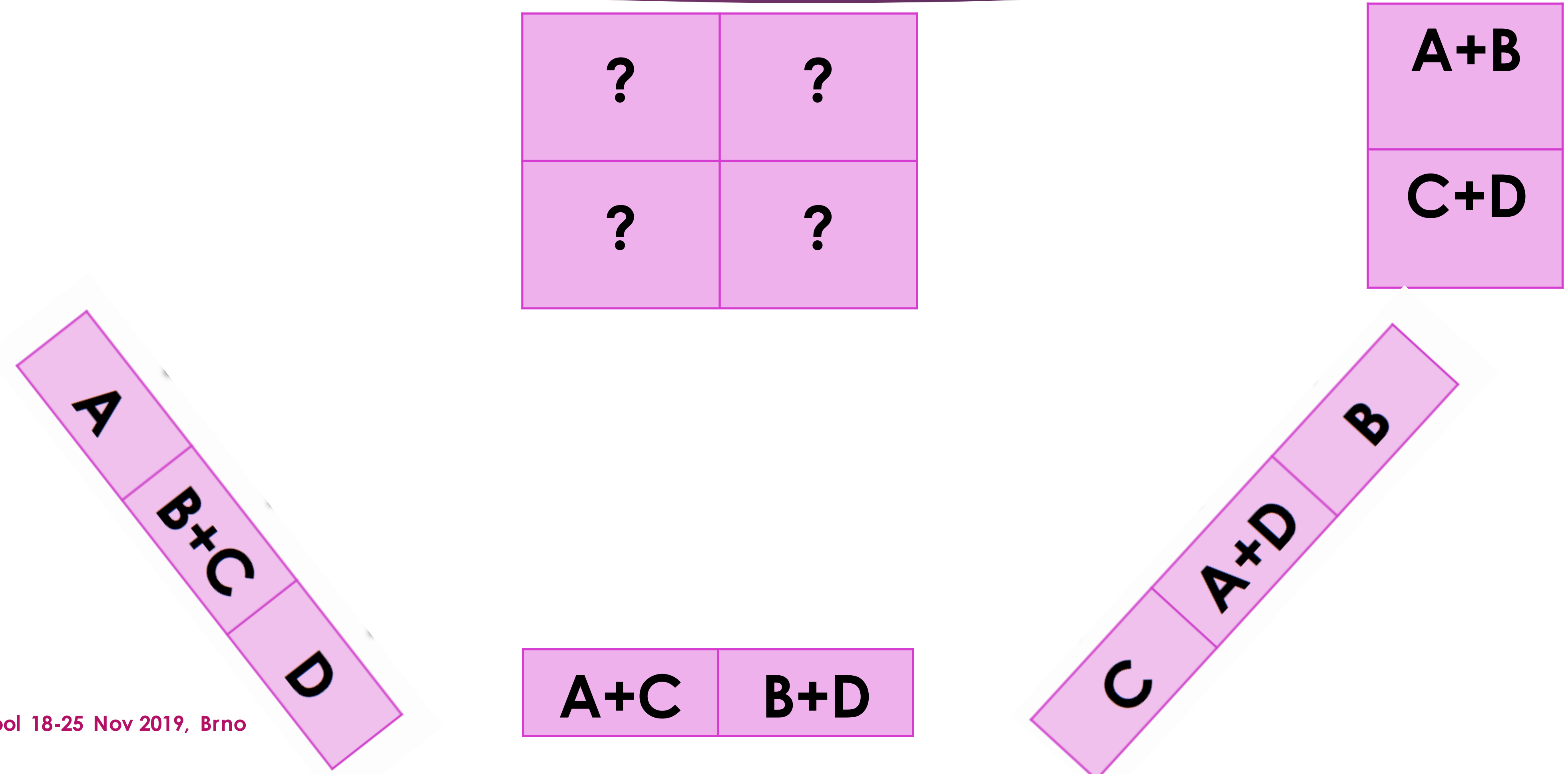

Numeric Reconstruction: algorithm

- backproject all projections
- subtract the sum of a projection (the same for all)
- divide by the number of projections

Numeric Reconstruction: image

$\Sigma = A + B + C + D$

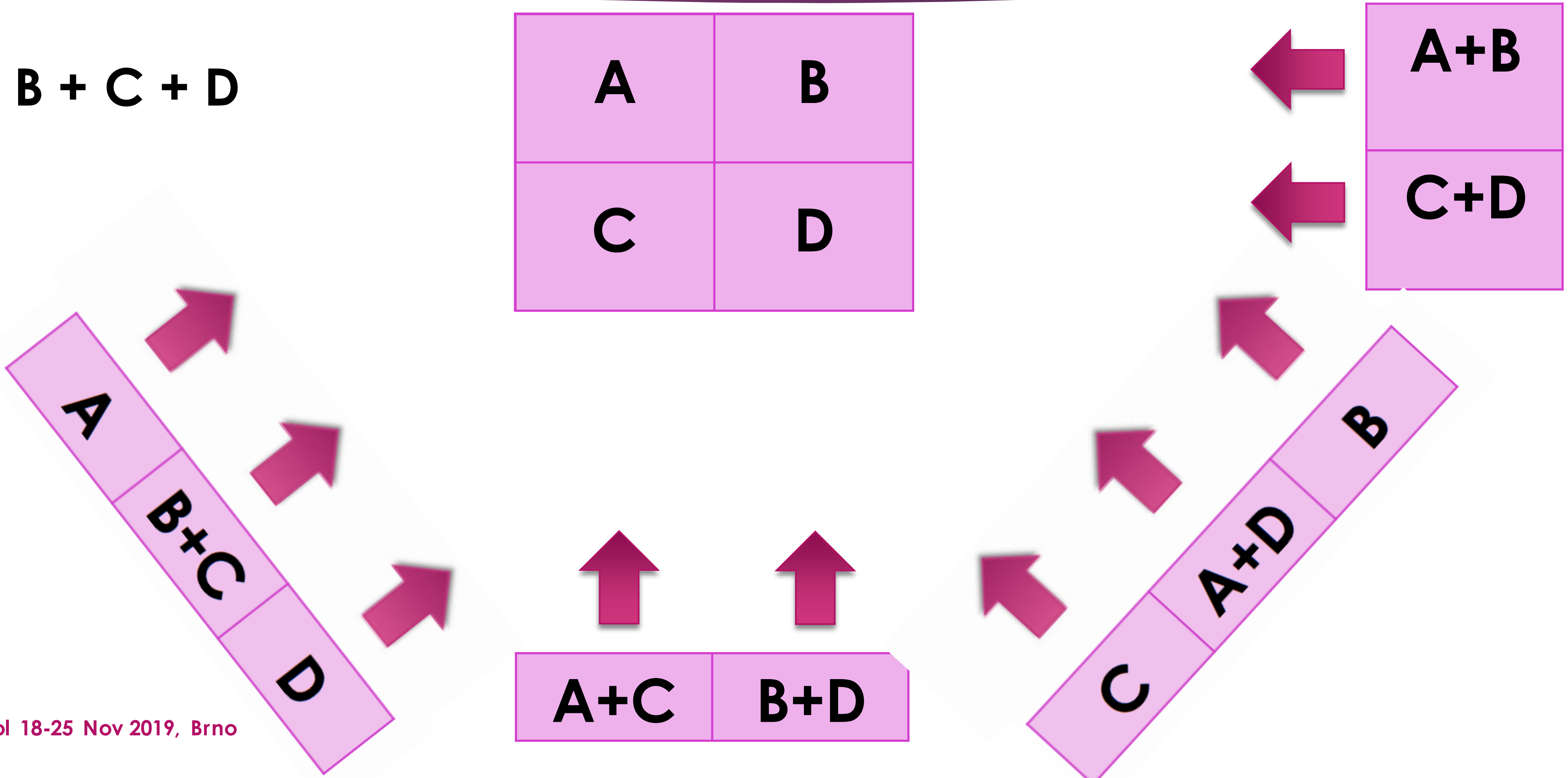

Backprojection vs filtered backprojection

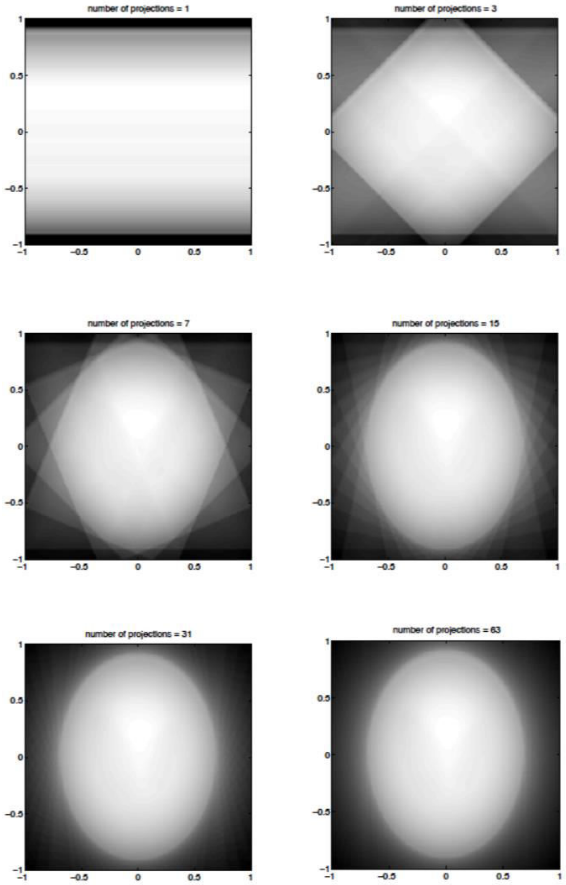

Backprojection overemphasize low frequencies

Ramp filter has to be applied to projections for exact image reconstruction

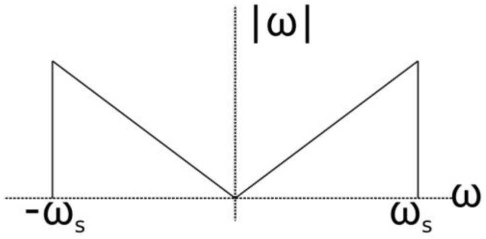

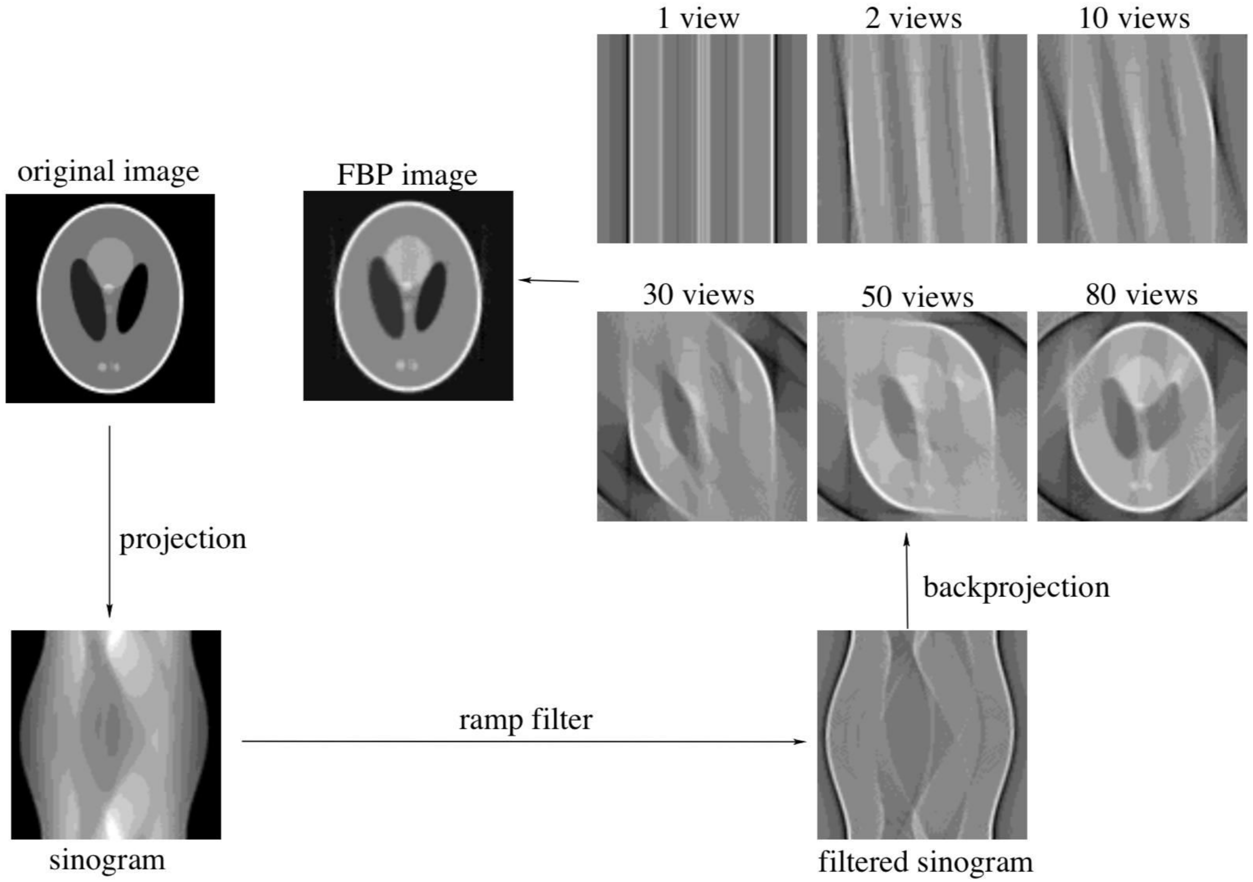

Image Reconstruction

- For exact image reconstruction infinite number of projection has to be acquired (continuous case).
- For discrete image represented by matrix of N^3 voxels, number of projections is given by Nyquist theorem, $\sim 4\pi N^2$ (still very large).
- For practical imaging, reduced number of projections that delivers "sufficient" image quality is taken (typically 10x times lower)
- Filtered backprojection is the facto standard for spatial domain image reconstruction
- The variety of algebraic and iterative reconstruction methods for space and k-space data has been developed
- Sparse image acquisition techniques are developed. Those allow to have less projections for comparable image quality but require long computation times.

FID of a Sample in the Gradient Field

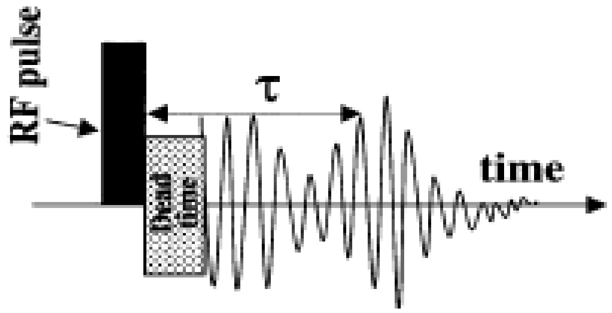

$$S(t) = \int_V f(\mathbf{x})\, e^{i\gamma_e (B_0 + \mathbf{G}\mathbf{x})t}\, d\mathbf{x}$$

- no relaxation
- static gradient

$$\mathbf{k} = \frac{\gamma_e}{2\pi}\mathbf{G}t$$

Pulse EPR signals represent object’s k-space

Radial k-space sampling

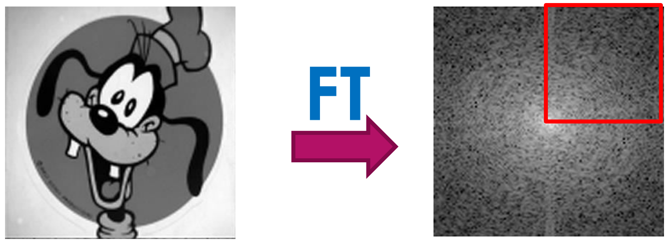

$$S(t,\mathbf{G}) = \int_V f(\mathbf{x}) e^{i\gamma_e \mathbf{G}\mathbf{x}t} d\mathbf{x}$$

Spin echo

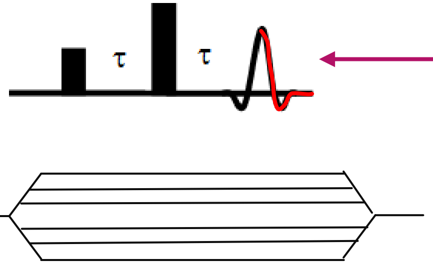

'Static' gradients

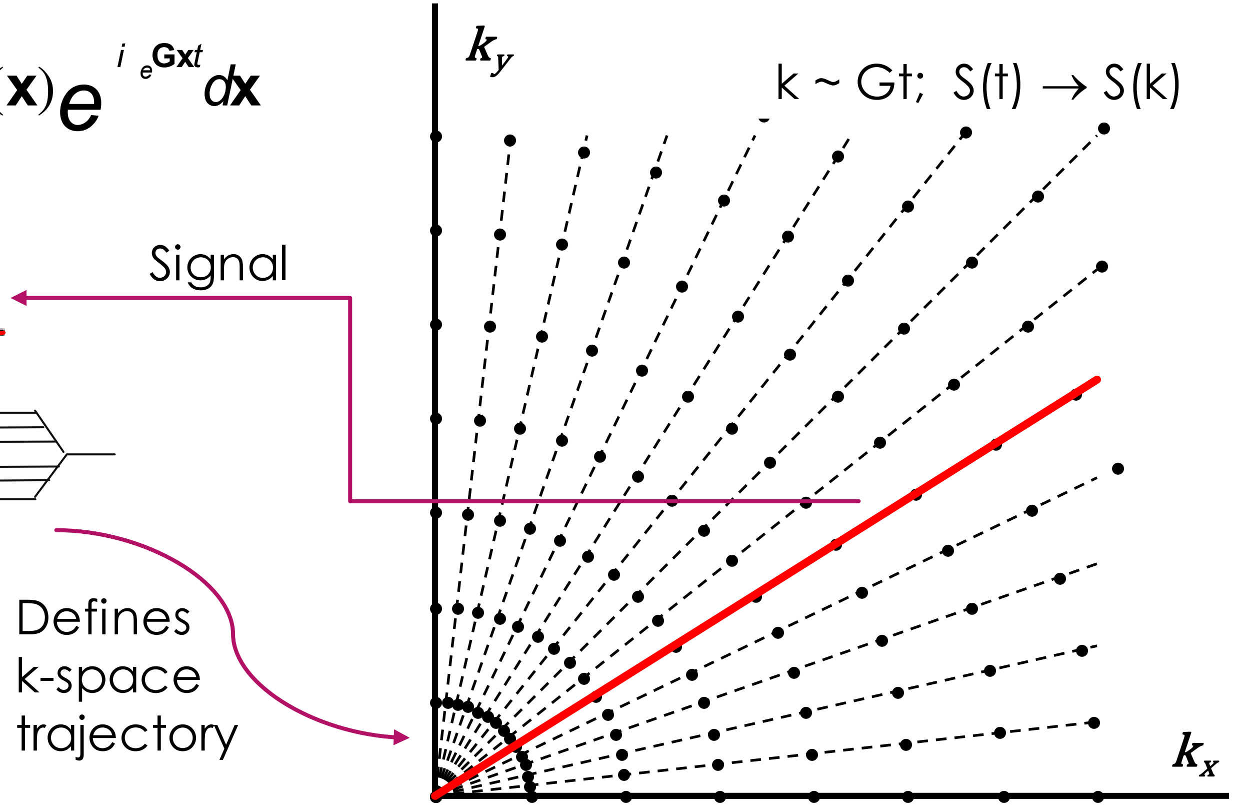

- +Fast
- +Easily combined with many pulse sequences
- -Relaxation limits image quality
- -Non-uniform k-space sampling

Inversion Recovery (IRESE) – T_1 Imaging

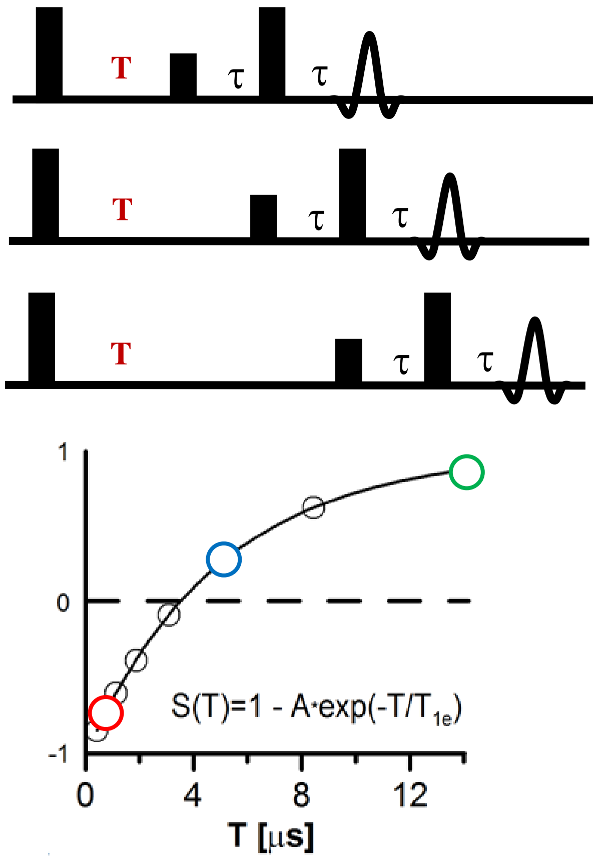

3D images
for each delay

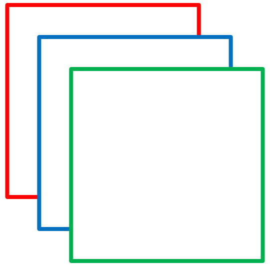

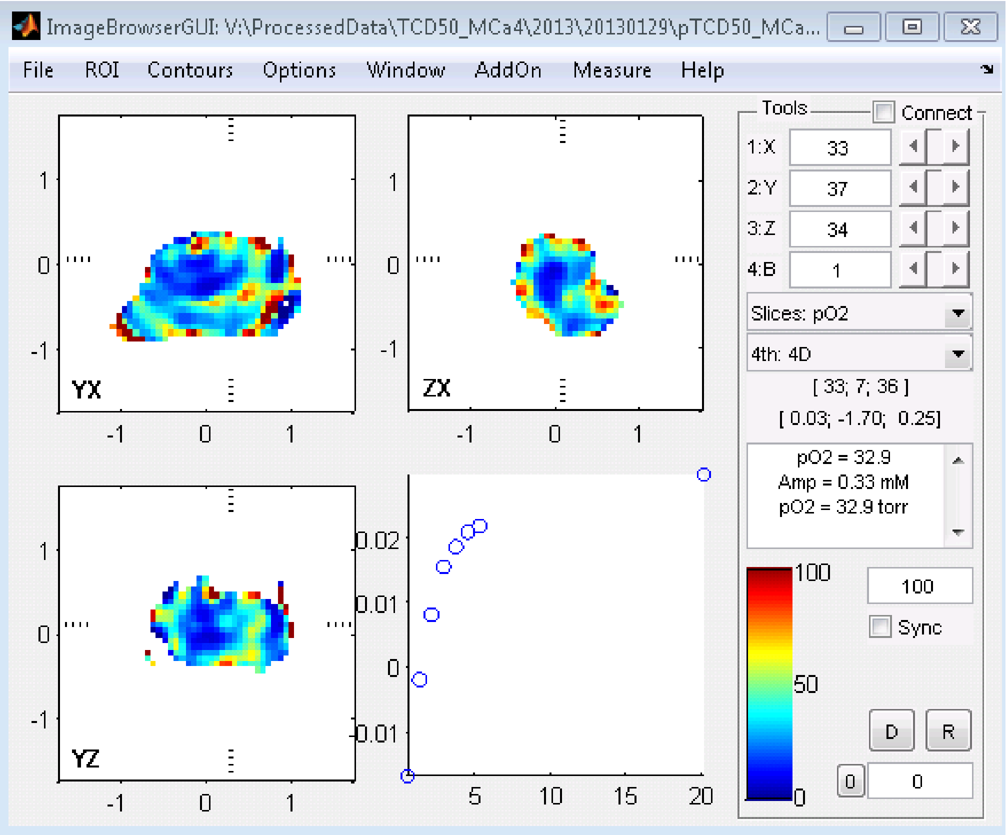

T_1 Sequences for ESE imaging

Saturation by fast repetition (SFR)

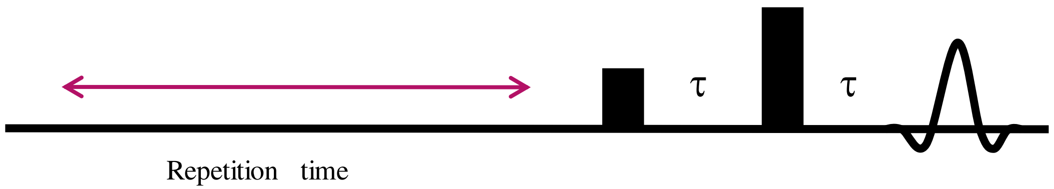

Inversion recovery (IRESE)

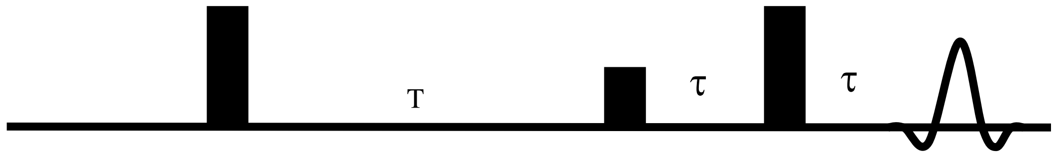

Stimulated Echo (SE)

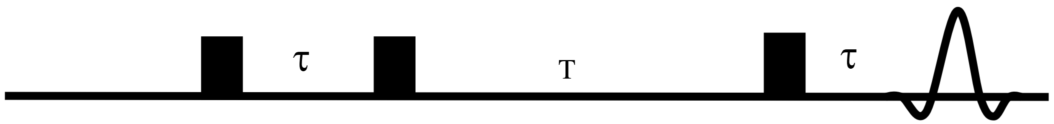

Spin echo is used to generate projections in all cases.

The same gradients are used for all sequences

Pulse Sequence	T_1	Error of T_1
SFR	6.2 μs	1.4 μs
IRESE	**5.9 μs**	**0.29 μs**
SE	5.8 μs	0.38 μs

At non-imaging conditions T_1 = 5.8 μs

pO_2 images: T2 vs T1 Relaxation

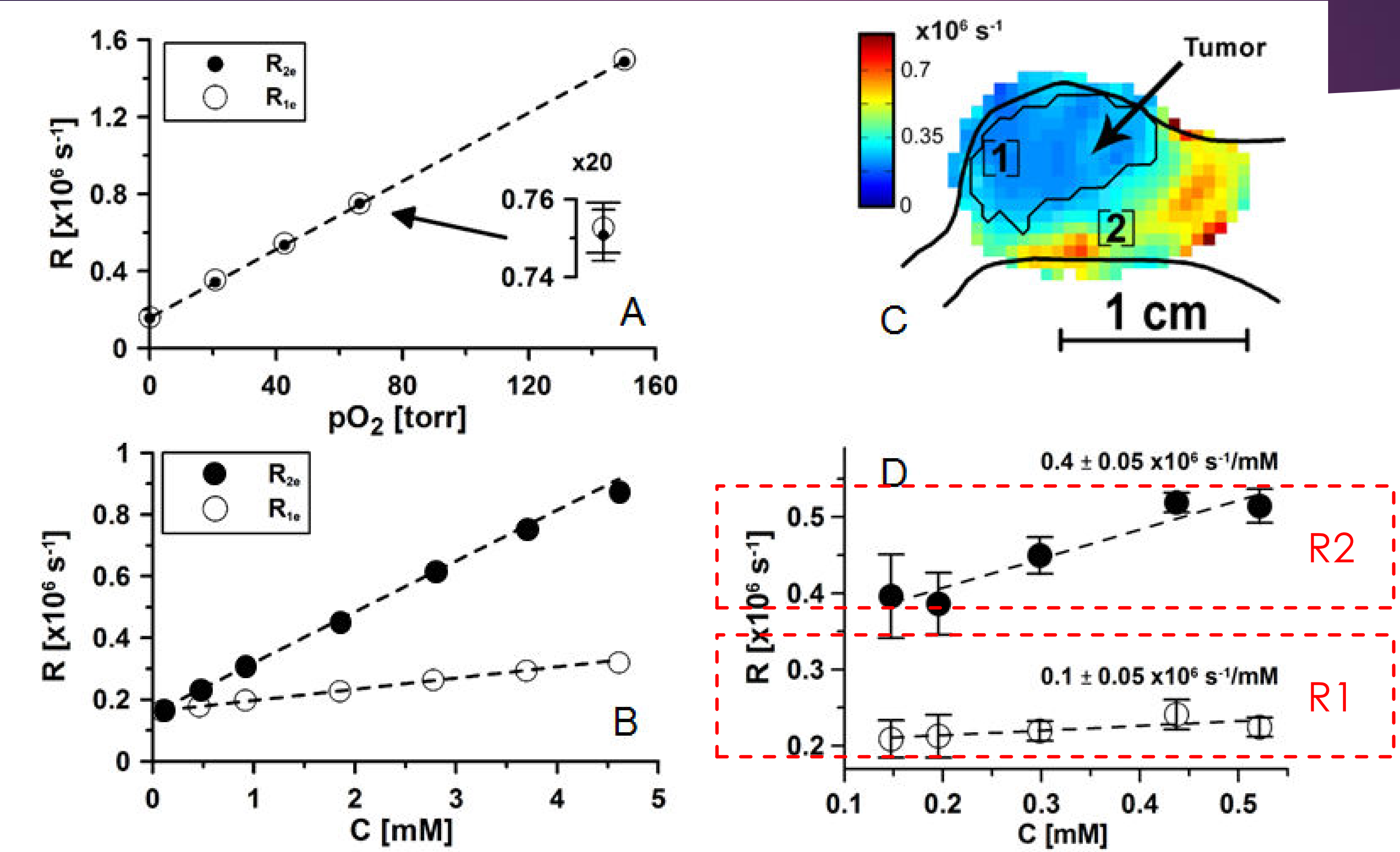

T1 imaging offers absolute accuracy of pO2 measurements

Single Point Imaging

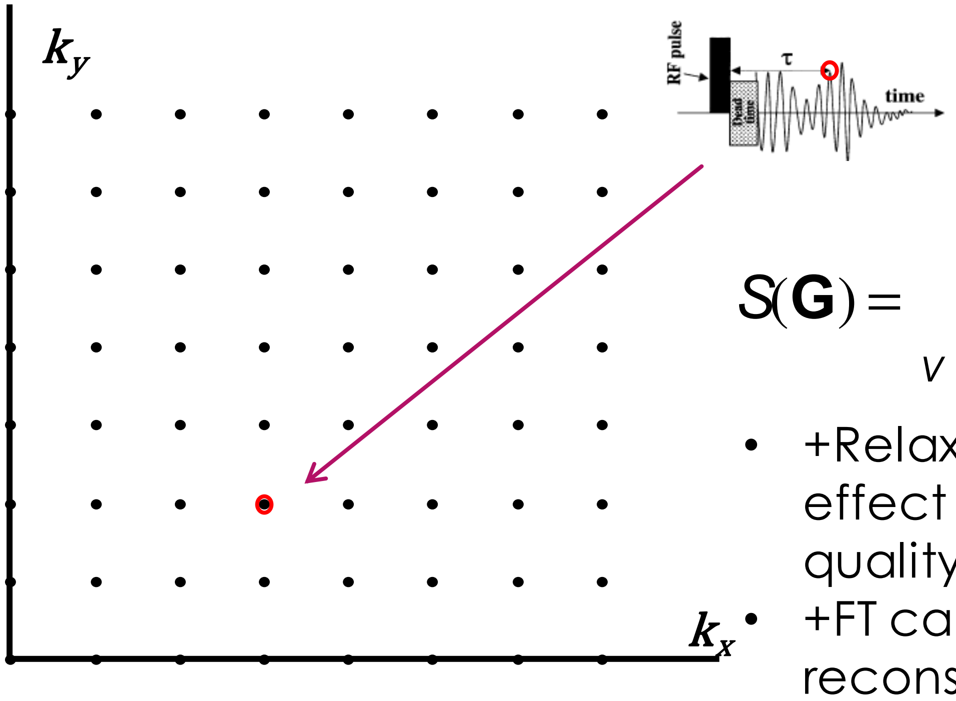

$$S(\mathbf{G}) = \int_V f(\mathbf{x}) e^{i\gamma_e \mathbf{G}\mathbf{x}}\, d\mathbf{x}$$

- +Relaxation has no effect on image quality
- +FT can be used for reconstruction
- -Slow

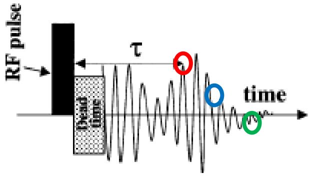

(G,τ_1), (G, τ_2), (G, τ_3)

(G_1,τ_1), (G_2, τ_2), (G_3, τ_3)

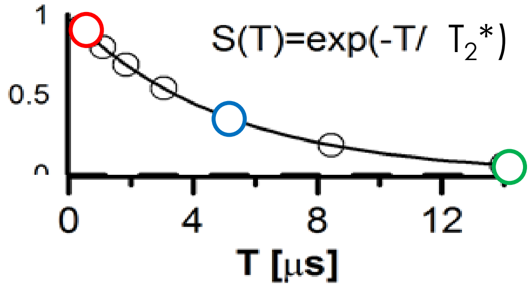

Idea: S. Emid and J. H. N. Creyghton, Physica B & C, 1985, 128, 81–83.

MRI - SPRITE JB Balcom et al JMR 136(2) (1999)159-168

EPR – SPI Subramanian, S., et al. Magn. Res. Med. 48(2) (2002) 370-379.

Development of *In vivo* Oxygen Imaging

CW(T_2^*) SPI(T_2^*) ESE(T_2) IRESE(T_1)

First pO_2 in vivo image

Halpern, H. J., C. Yu, et al. PNAS (**1994**) 13047-13051.

Single Point Imaging

Subramanian, S., et al. Magn. Res. Med. 48(2) (**2002**) 370-379.

T1 in vivo imaging

B. Epel et al. (**2014**). Magn Reson Med 72: 362-368.

First in vivo pO2 ESE image

B. Epel et al. Concepts in Magn. Reson. Part B 33B (**2008**) 163-176.

Spectral-spatial imaging methodology

M.M. Maltempo et al. JMR 72 (**1987**) 449-455.
P. Kuppusamy et al. PNAS 91 (**1994**) 3388-3392.

First pulse measurements on trityls

Murugesan, R., et al. Magn. Res. Med. 38(3) (**1997**) 409-414.

Electron Spin Echo Imaging

C. Mailer et al. Magnetic Resonance in Medicine 55 (**2006**) 904-912.

EPR in vivo Imaging

In vivo EPR spectroscopy and imaging methods enable noninvasive mapping of tissue pO_2.

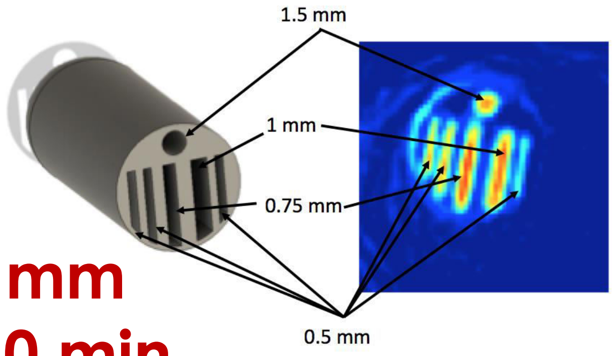

Mouse Carbogen Challenge
(1 minute resolution)

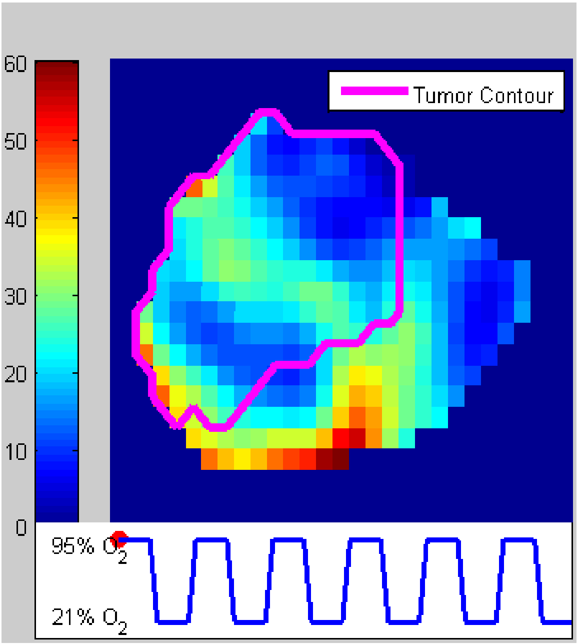

Image resolution

spatial resolution	**~1 mm**
temporal resolution	**1-10 min**
pO_2 resolution	**1 torr**

Imaging with static gradients

Application:
in vivo

Low frequencies (<1 GHz)
Large objects

Continuous wave Methodologies

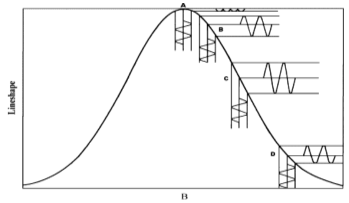

Field modulation, first harmonic detection

Halpern HJ, Spencer DP, Vanpolen J, Bowman MK, Nelson AC, Dowey EM, Teicher BA. Rev Sci Instrum 1989;60(6):1040-1050. Kuppusamy P, Afeworki M, Shankar RA, Coffin D, Krishna MC, Hahn SM, Mitchell JB, Zweier JL. Cancer Research 1998;58(7):1562-1568.

Fast relaxing probes

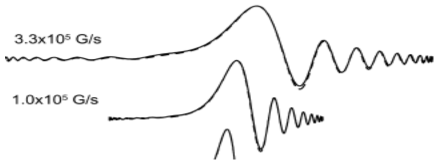

Rapid Scan with direct detection

Stoner JW, Szymanski D, Eaton SS, Quine RW, Rinard GA, Eaton GR; J Magn Reson 2004;170(1):127-135.

Pulse Methodologies

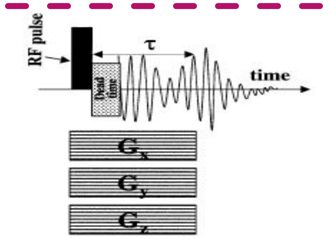

Single Point Imaging

Subramanian S, Devasahayam N, Murugesan R, Yamada K, Cook J, Taube A, Mitchell JB, Lohman JAB, Krishna MC. Magnet Reson Med 2002;48(2):370-379.

Slow relaxing probes

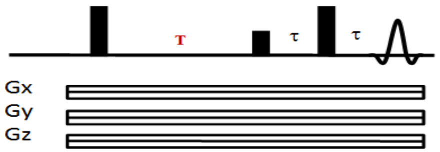

Spin Echo Imaging

Mailer C, Sundramoorthy SV, Pelizzari CA, Halpern HJ. Magnet Reson Med 2006;55(4):904-912. Epel B, Bowman MK, Mailer C and Halpern HJ, 2013; MRM under revision.

Microscopy - Imaging with Pulse Gradients

Application:
Material science

High frequencies
(K-band and up)
Small objects

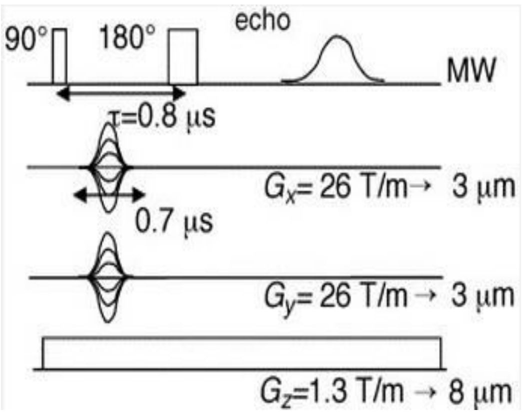

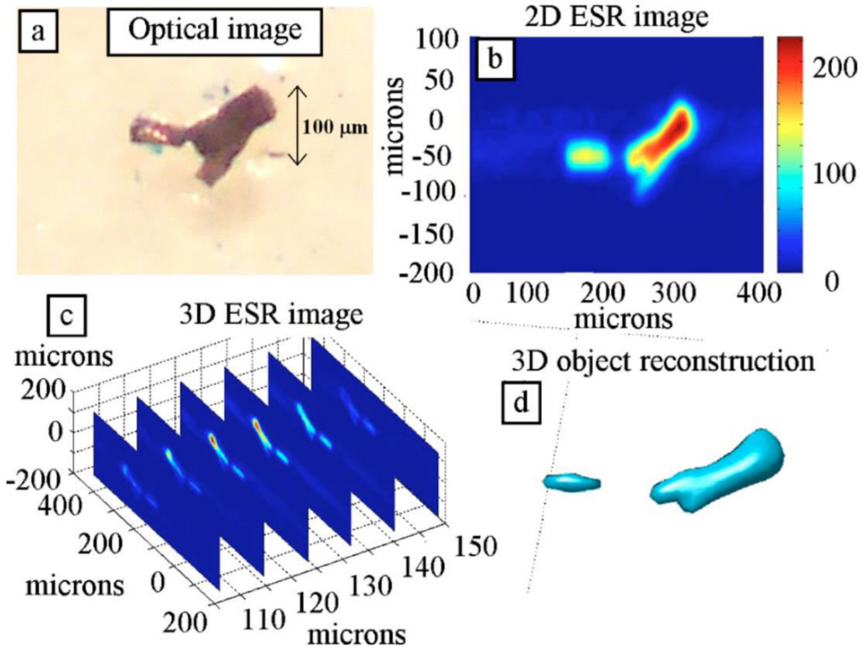

Gradient pulse duration must be shorter than EPR signal phase relaxation - gradient coils of any substantial size would consume too much power

Blank, A., C. R. Dunnam, P. P. Borbat and J. H. Freed (2004). Applied Physics Letters **85**(22): 5430-5432.

The University of Chicago

Center for EPR Imaging in Vivo Physiology

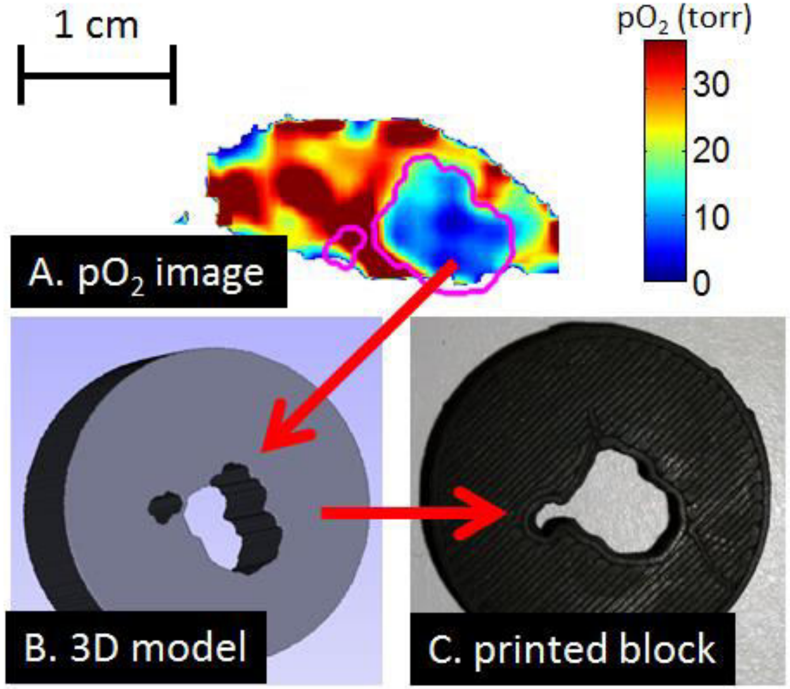

Oxygen-guided radiation therapy

OXYGENATION AS A THERAPY TARGET

Hypoxic fraction predicts radiotherapy outcome

cervix, Hockel 1996

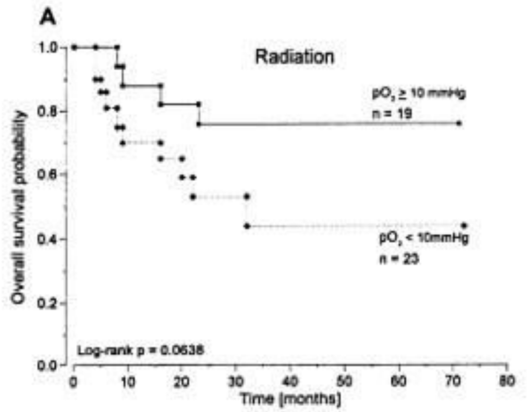

head and neck, Nordsmark 1996

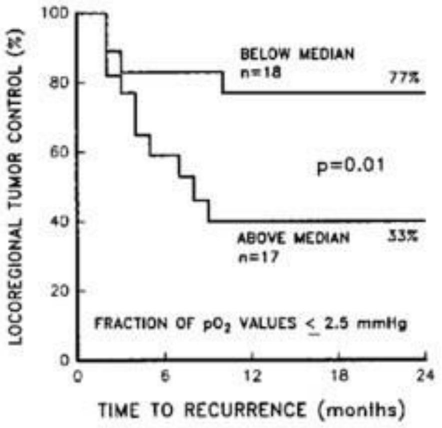

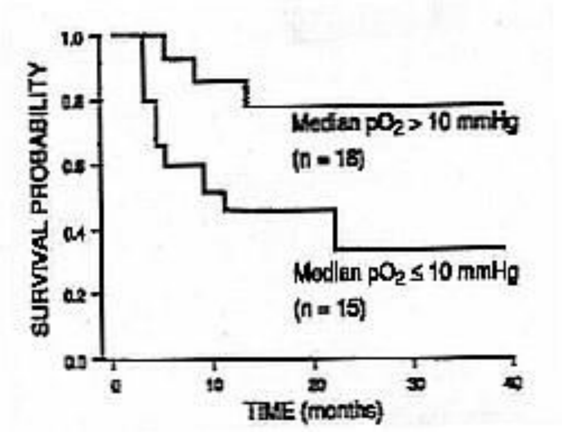

Electrode

Animal models, FSa, MCa4 tumors. Elas 2011, 2013

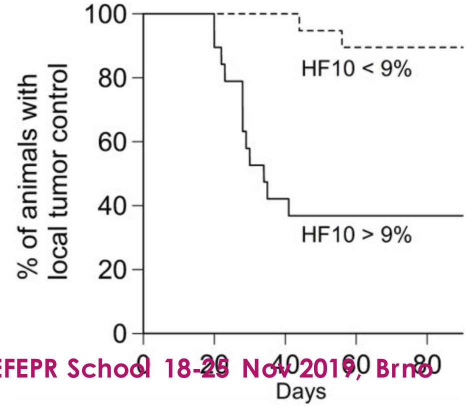

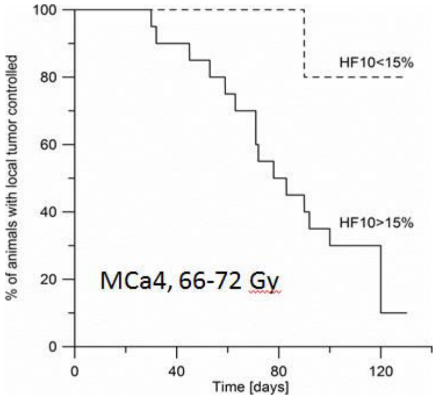

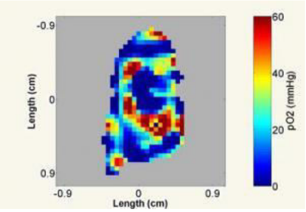

EPR pO2 imaging

Can we use oxygen knowledge to improve the treatment?

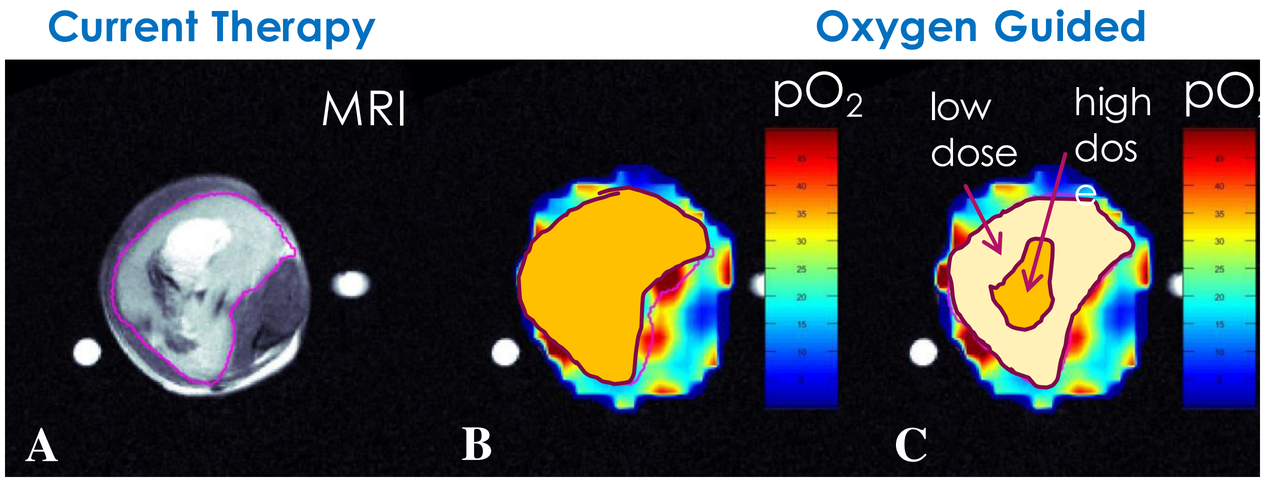

Oxygen-guided RT experiment

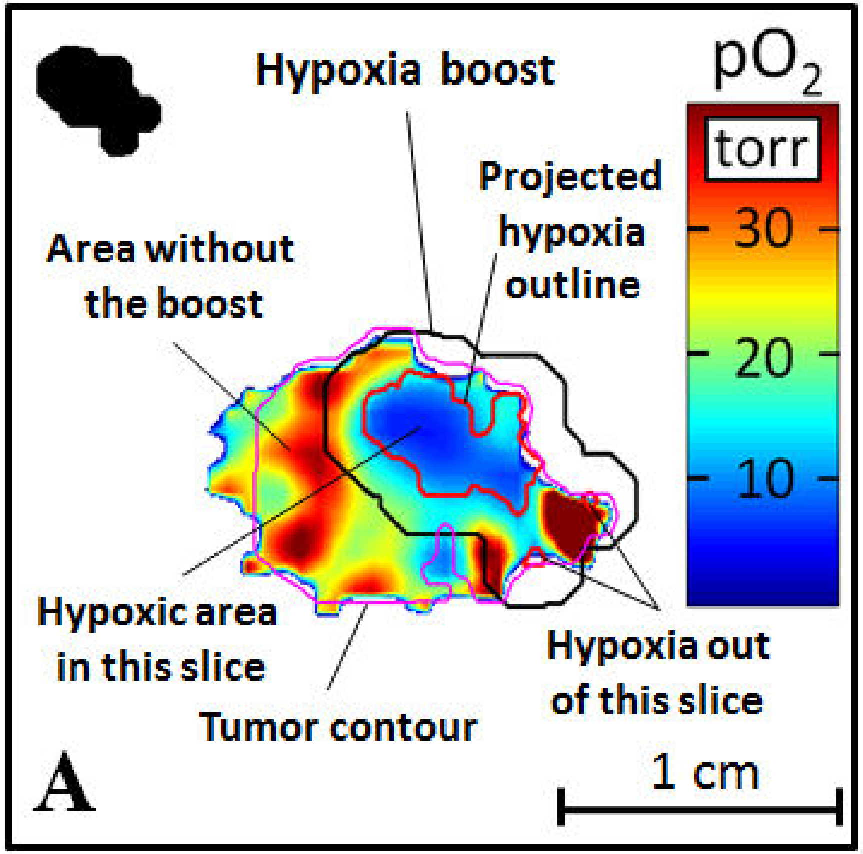

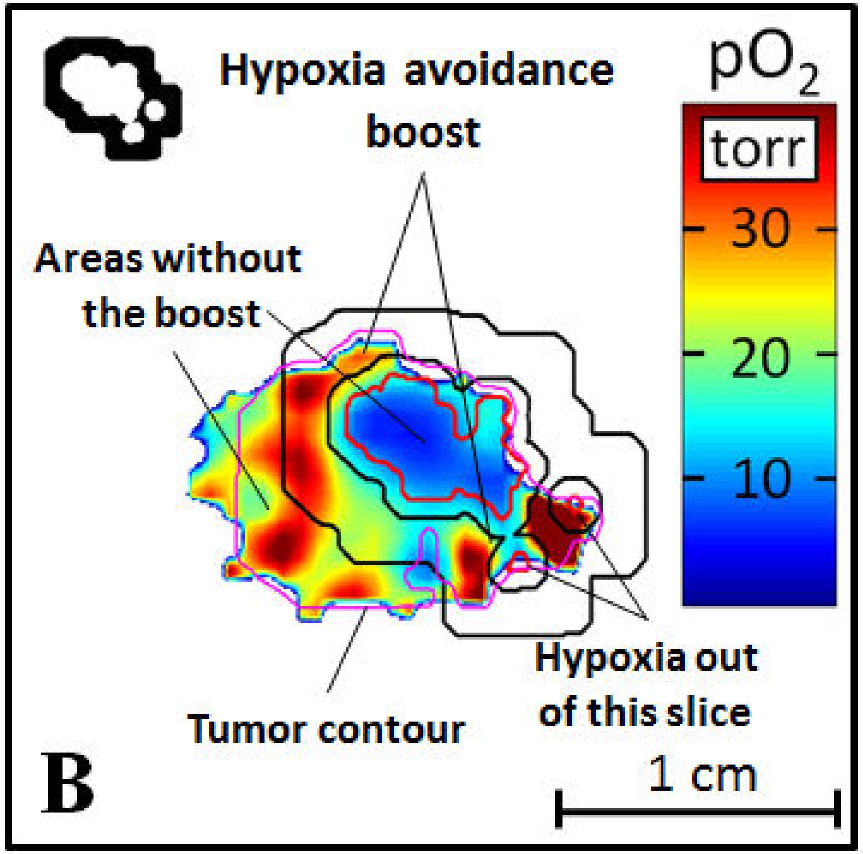

A. Treat hypoxic volumes with full dose and normoxic volumes with much lower dose

B. Control. Treat normoxic volumes with full dose and hypoxic volumes with much lower dose

Radiation delivery with sub-millimeter precision

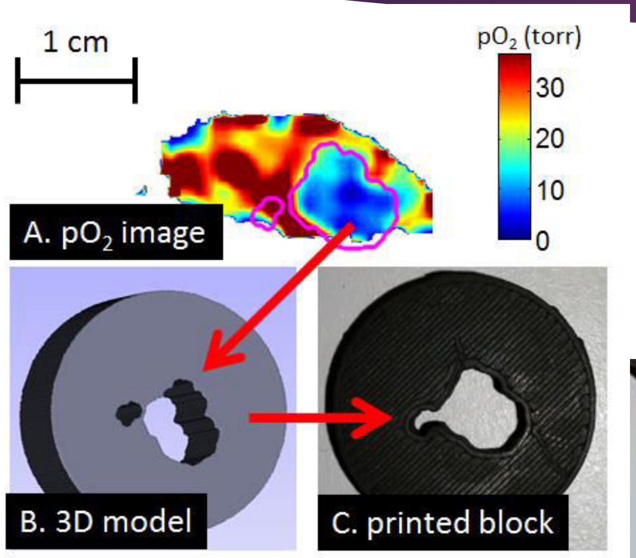

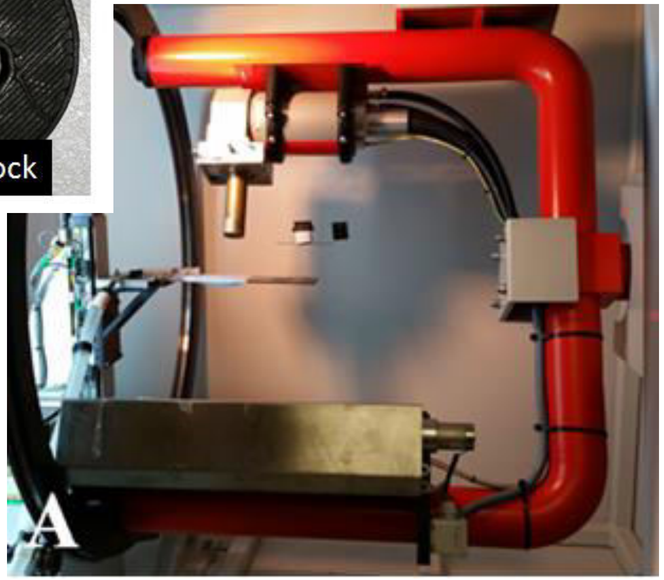

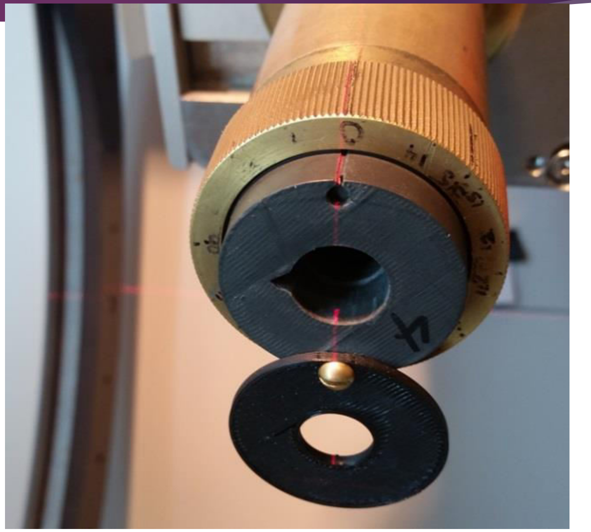

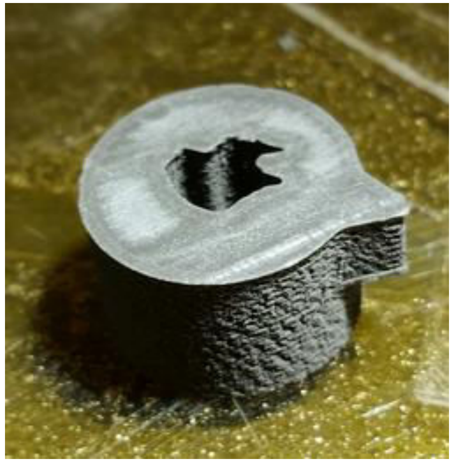

Hypoxia boost treatment showed efficiency in two cancer models

NV = volumes pO2 > 10

HV = volumes pO2 ≤ 10

▶Hypoxia Boost:

TCD15 applied to NV

TCD95 applied to HV

▶Hypoxia Avoidance:

TCD15 applied to HV

TCD95 applied to NV

Fsa tumors

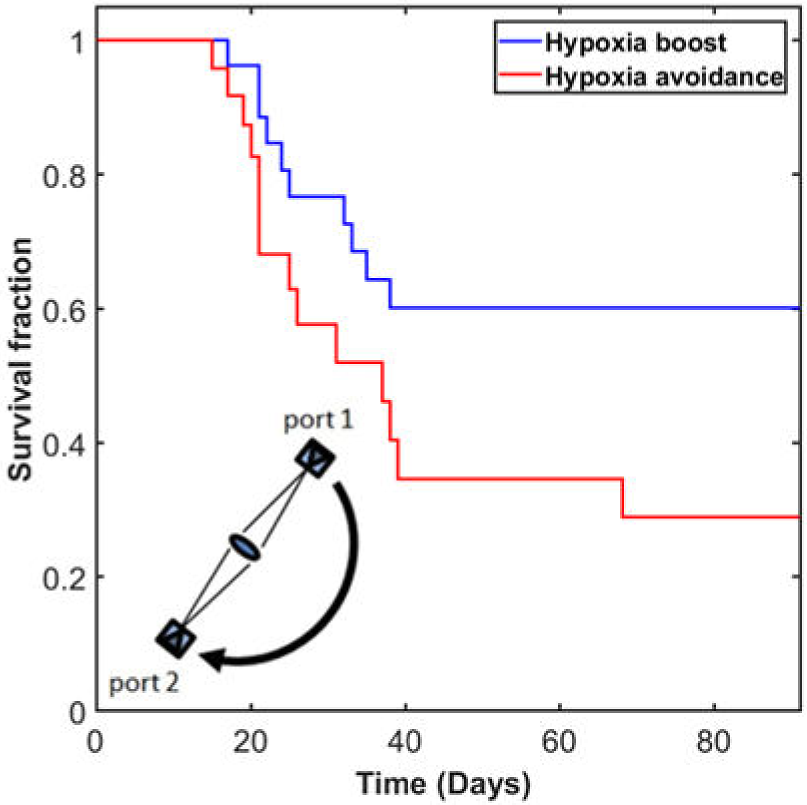

MCa4 tumors

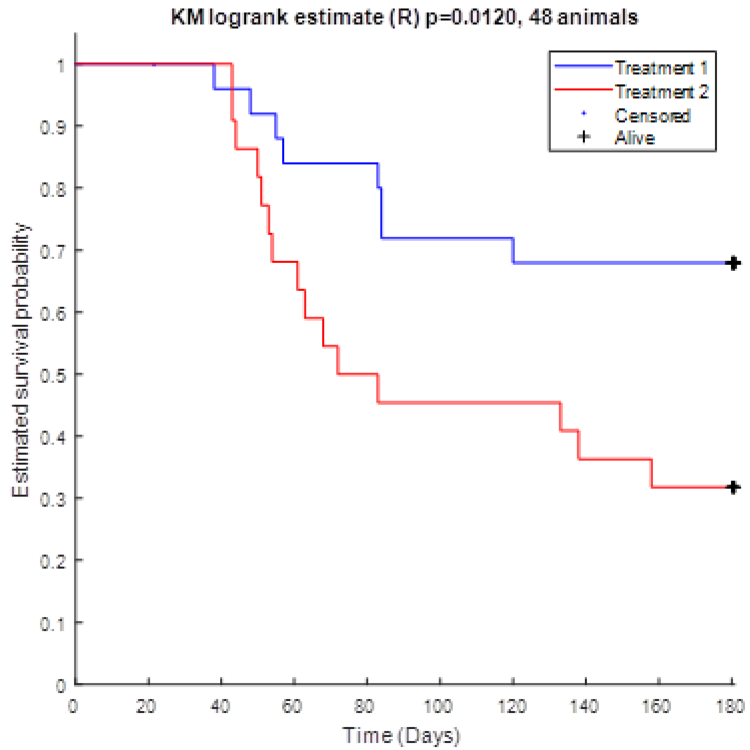

Epel, B. et al. (2019). "Oxygen-Guided Radiation Therapy." International Journal of Radiation Oncology Biology Physics **103**(4): 977-984.

GSH / redox imaging

- Thiol groups are reducing agents, existing at a concentration around 5-10 mM in animal cells.
- Glutathione (GSH) is an important antioxidant preventing damage to important cellular components caused by reactive oxygen species (ROS) such as free radicals, peroxides and heavy metals.
- The GSH/GSSG couple constitutes close to half of the thiol/disulfides in the cell, and is thus considered to be the principal redox buffer.
- In malignant tumors, the resistance to radiation and chemotherapy is associated with higher GSH levels.
- Redox images may assist in better treatment planning

Reaction of GSH and PxSSPx spin probe

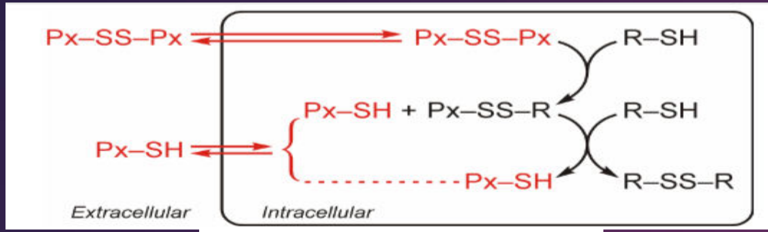

R = Glutathione

GSH

PxSH

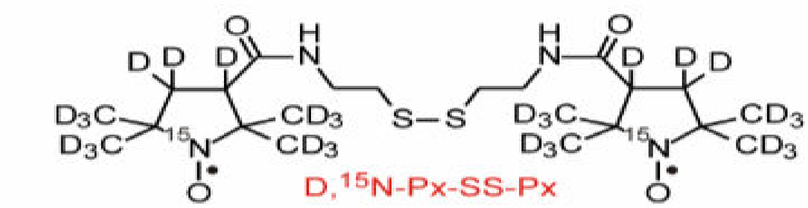

+

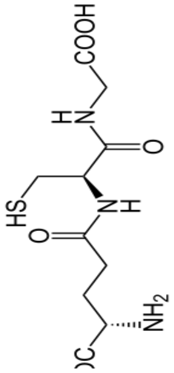

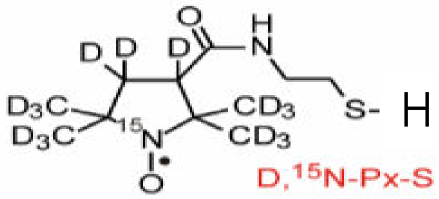

GSSG

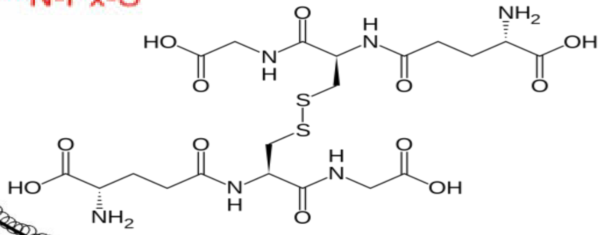

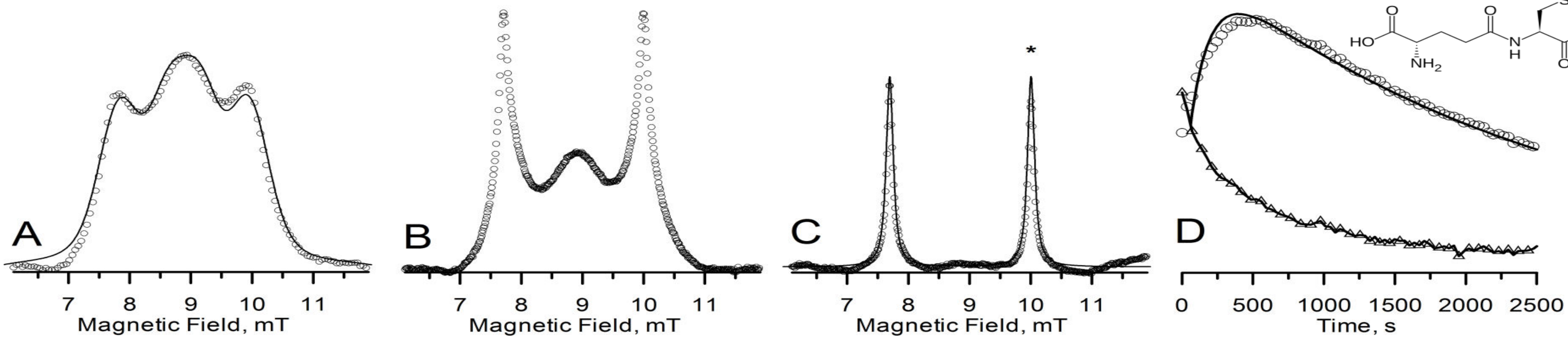

PxSSPx Spin Probe in vivo

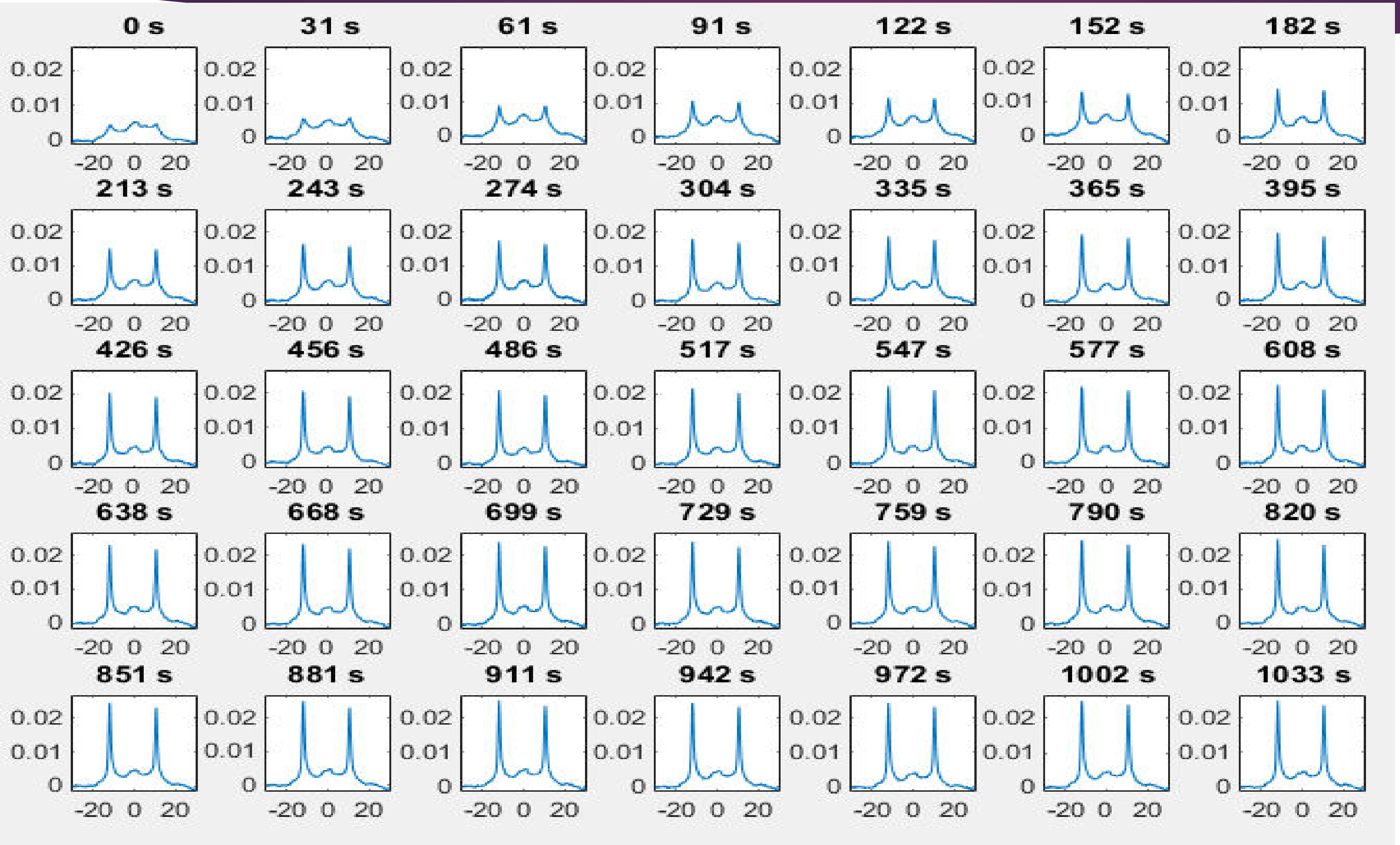

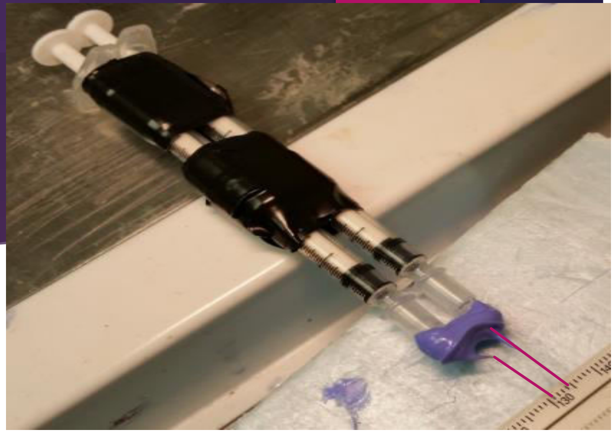

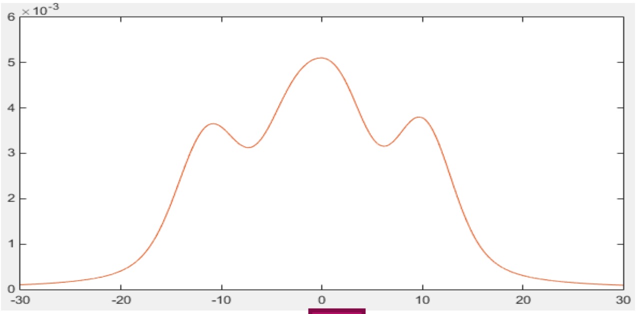

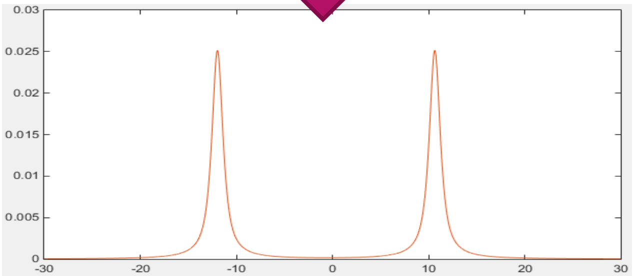

GSH imaging

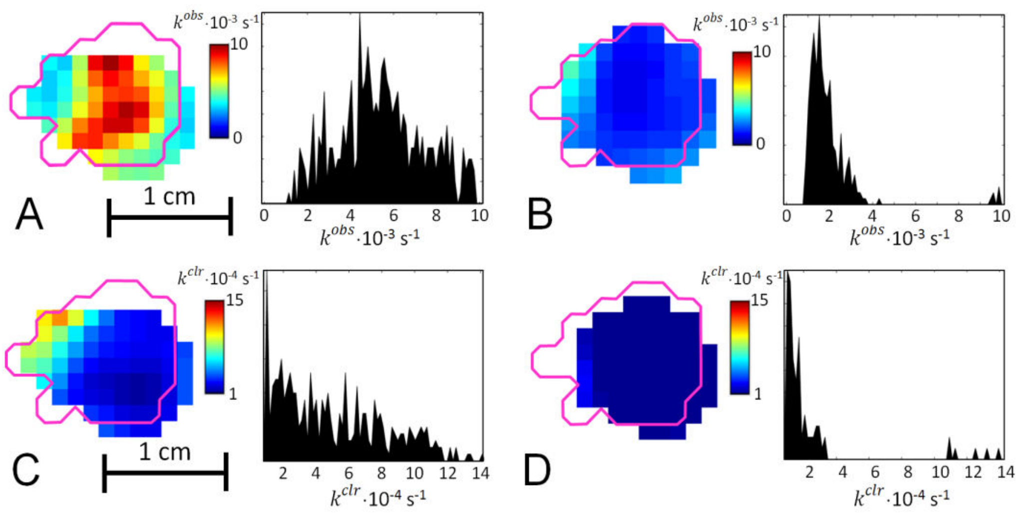

$S_{PxSH}=aS_{PxSSPx}(1-e^{-kobs\ t})e^{-kclr\ t}$

Tumor treated with BSO (*L*-buthionine sulfoximine, a specific inhibitor of GSH biosynthesis)

Epel, B., S. V. Sundramoorthy, M. Krzykawska-Serda, M. C. Maggio, M. Tseytlin, G. R. Eaton, S. S. Eaton, G. M. Rosen, J. P. Y. Kao and H. J. Halpern (2017). JMR **276**: 31-36.

O2M Technologies, LLC

Biomaterials

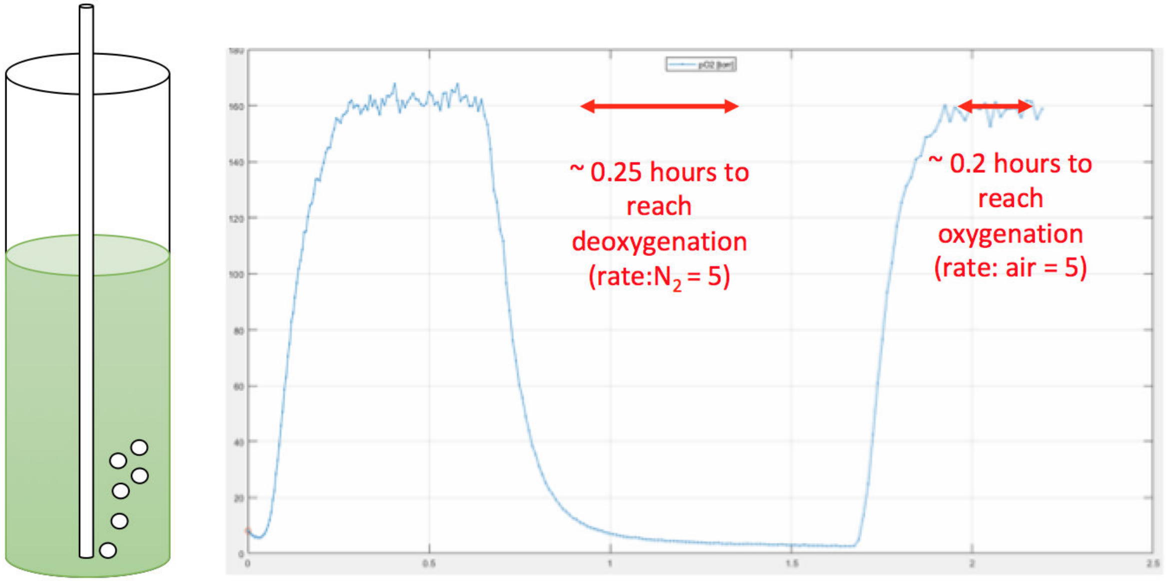

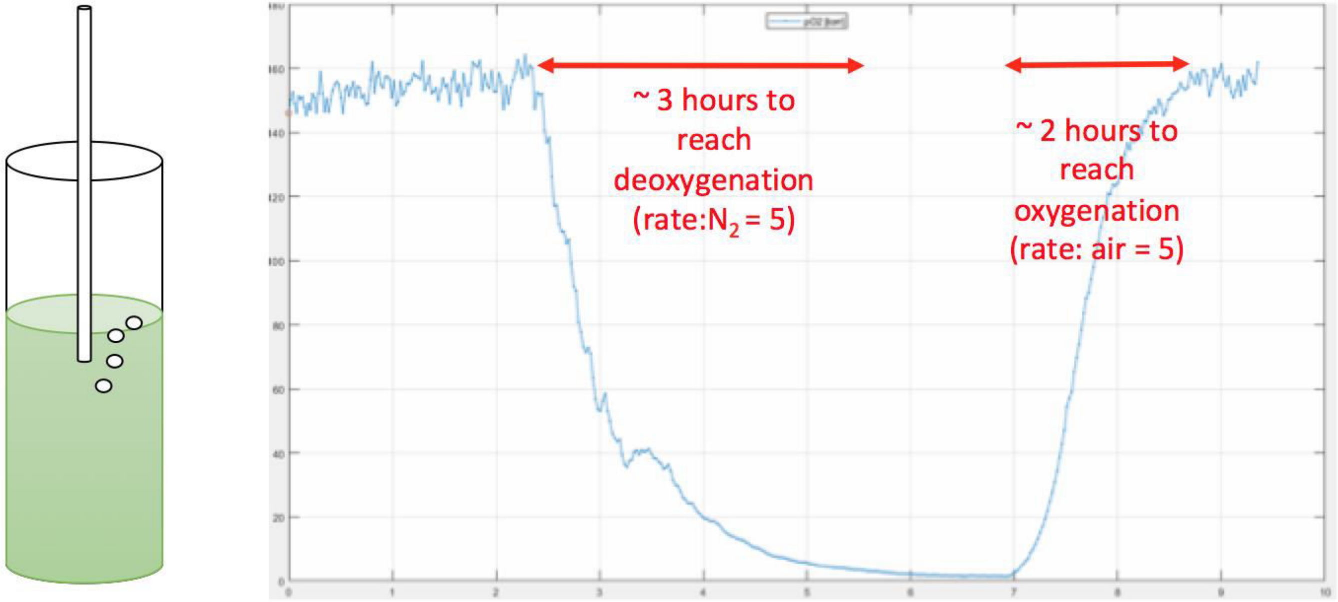

Effect of Porosity on pO_2 Concentration in PLGA-based bone grafts

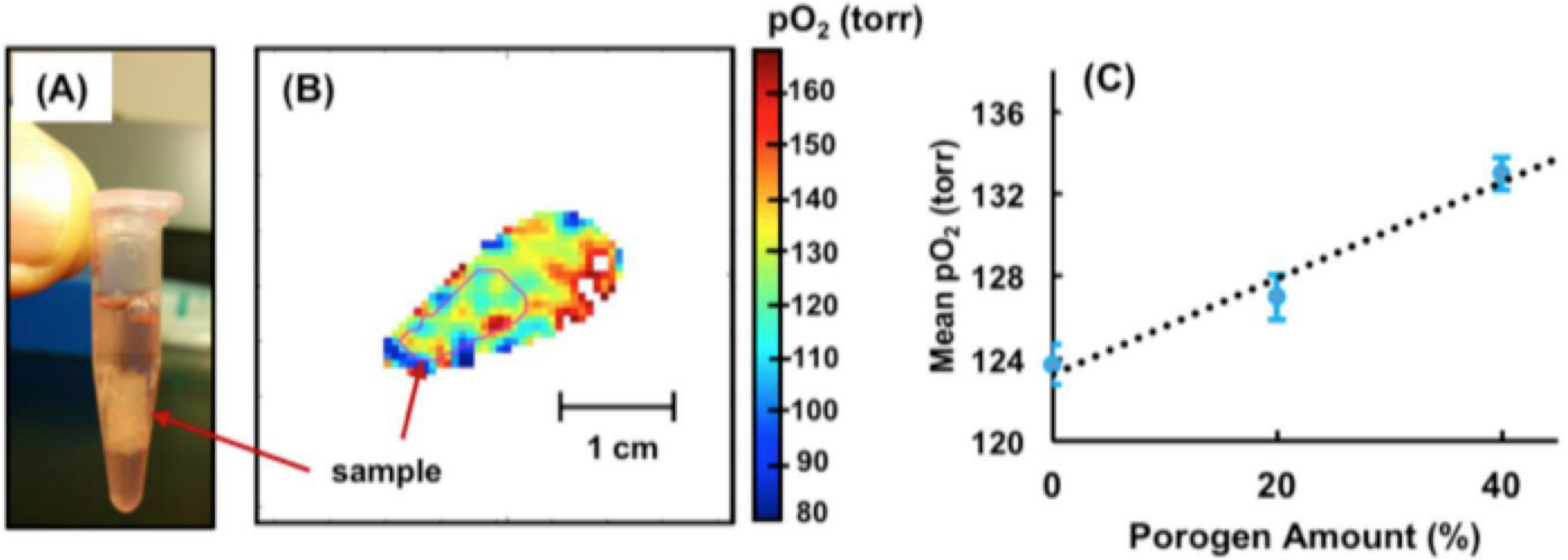

10 mm x 5 mm
sample size

pO_2 in Oxygen Deprivation Experiment

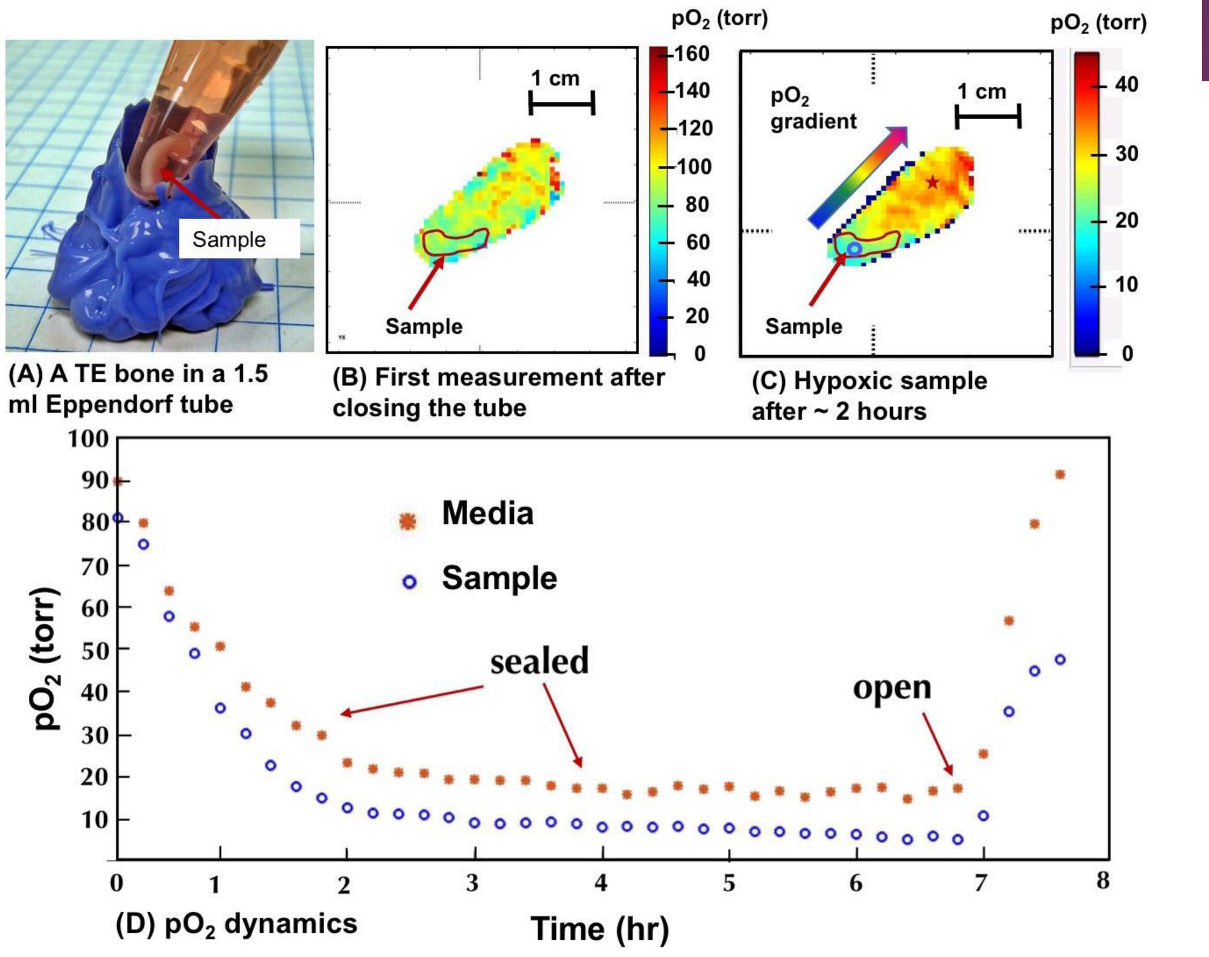

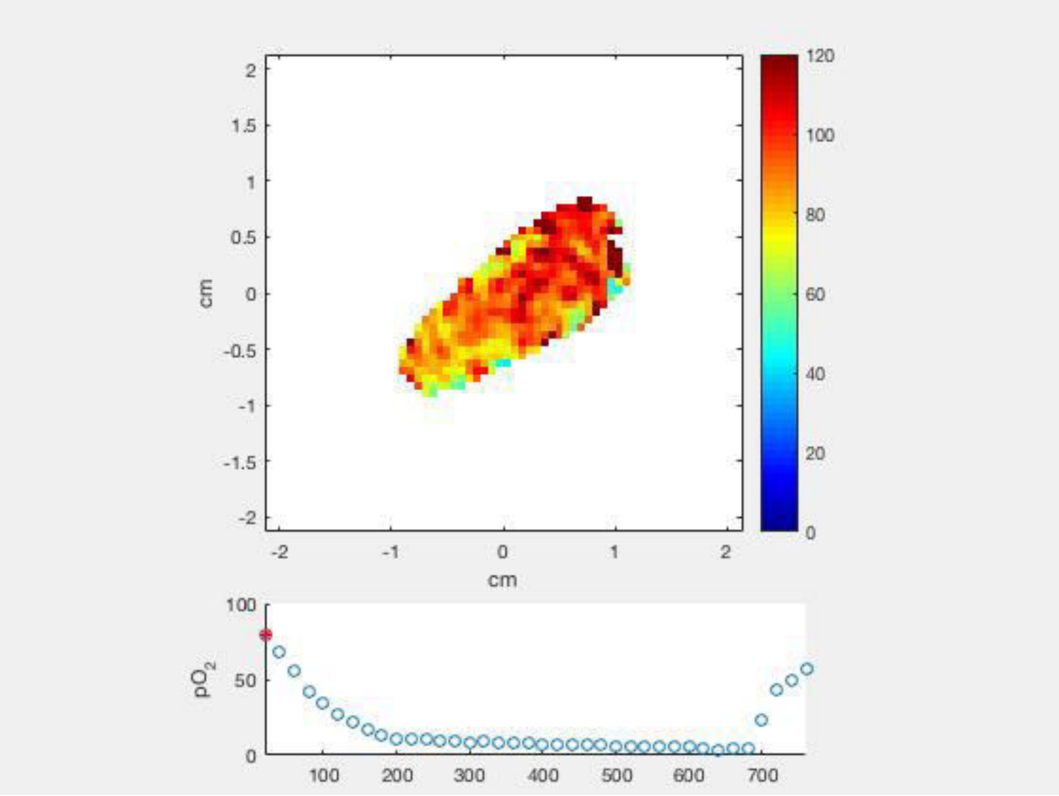

Sample: HMSCs seeded artificial bone

The University of Chicago

Center for EPR Imaging in Vivo Physiology

Spectral-Spatial Imaging

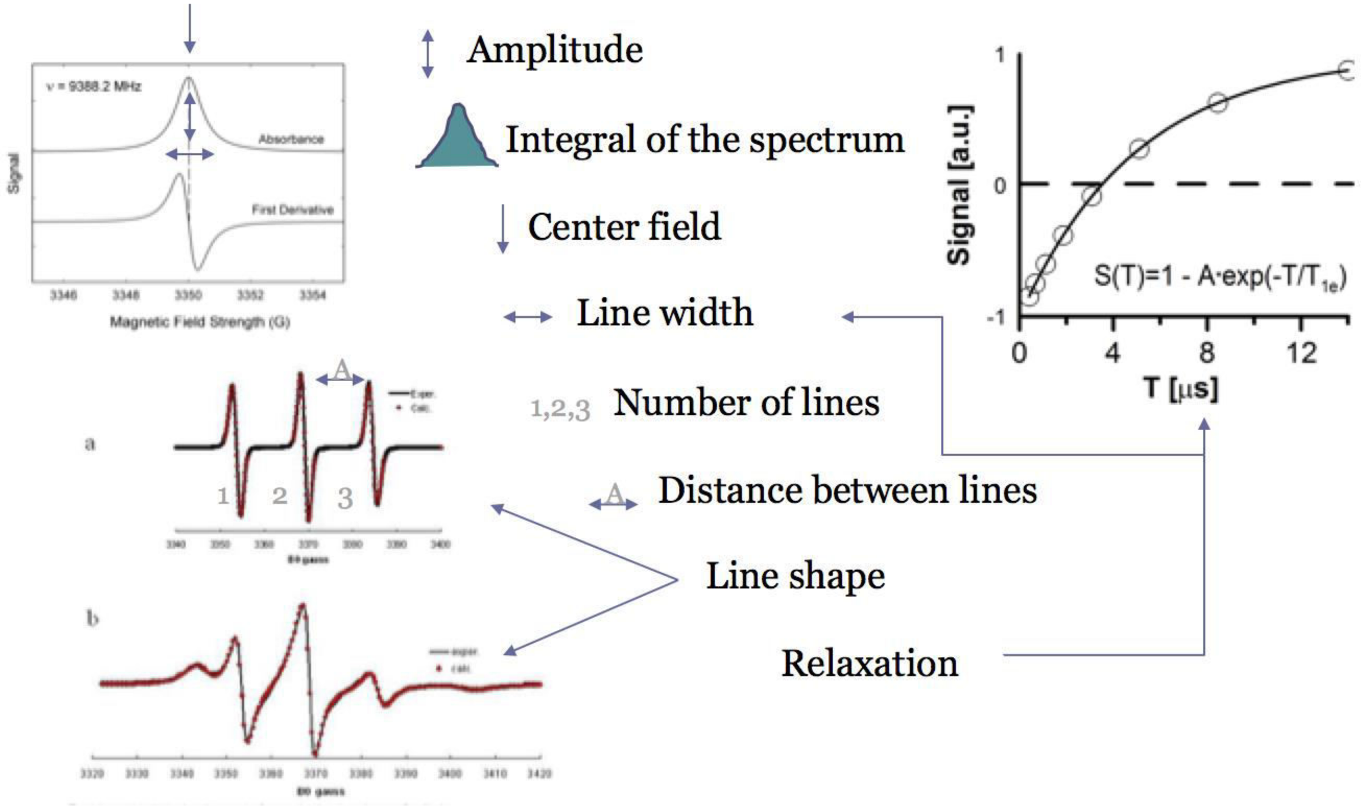

Spectral-spatial imaging explained

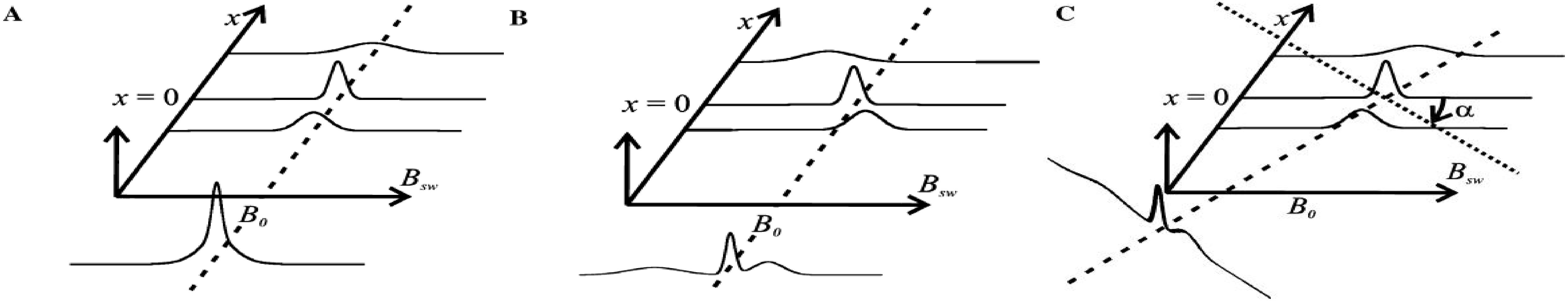

tan(α) = G dL / dB

Williams BB, Pan XC, Halpern HJ.. J Magn Reson 2005;174(1):88-96.

Change of the **gradient amplitude** in spectral-spatial image is mathematically equivalent to the rotation of the **projection direction** in spectral-spatial image.

Combination of 3D spatial and spectral acquisition gives a **4D spectral-spatial** image in which EPR line shape is measured in every spatial location.

EPR signal

Integral over B

Spectral–spatial object, 4D EPR density

$$s(B_{sw},\vec{G}) = \underbrace{\int_{B_0-\frac{\Delta B}{2}}^{B_0+\frac{\Delta B}{2}}}_{\text{Integral over B}} \underbrace{\int_{\Omega_{\vec{x}}}}_{\text{Integral over space}} \underbrace{f(B,\vec{x})}_{\text{Spectral–spatial object}} \underbrace{\delta(B-B_{app}(\vec{x}))}_{\text{Kronecker delta function}}\,\mathrm{d}\vec{x}\,\mathrm{d}B$$

Integral over space

Kronecker delta function

$$B_{app}(\vec{x}) = B_0 + B_{sw} + \vec{G}\cdot\vec{x}.$$

Williams, B. B., X. C. Pan and H. J. Halpern (2005). JMR **174**(1): 88-96.

Spectral Domain Acquisition

α_n, n=1 to N
$G_n = \tan(\alpha_n)\ dB/dL$
$B^{sw}{}_n = dB\ /\ \cos(\alpha_n)$

α – spectral angles between 0 and 90 degrees
dB – image support in spectral dimension [G]
dL – image support in spatial domain [cm]
$B^{sw}{}_n$ – field sweep required for projection

For multiple narrow line spectra, FBP protocol requires significant increase of dB to cover complete spectrum. This proportionally increase B^{sw} and G to unnecessarily large values

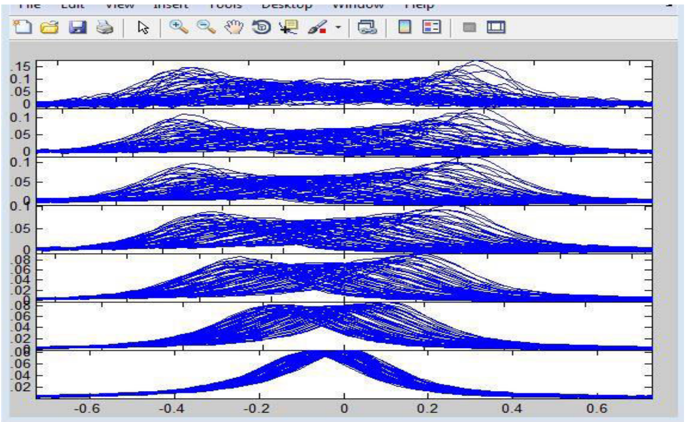

4D Spectral-Spatial Imaging

- Sampling the gradient volume using different gradients orientations and amplitudes
- Gradient vectors "fill the volume"
- EPR spectrum shape is obtained in every image voxel

- Pros:
  - *ALL information* about EPR spectra is collected
  - T2 can be extracted from line shape

- Cons:
  - Lower signal-to-noise ratio
  - Longer acquisition
  - T1 relaxation measurements are complicated

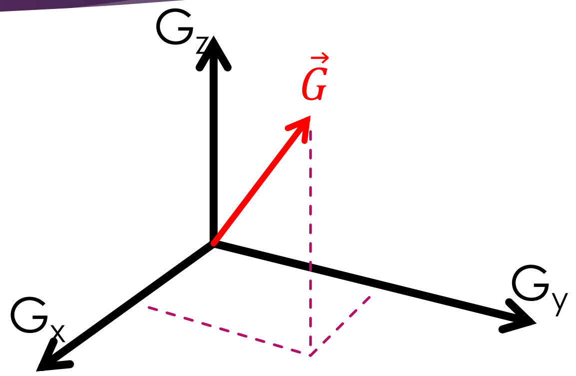

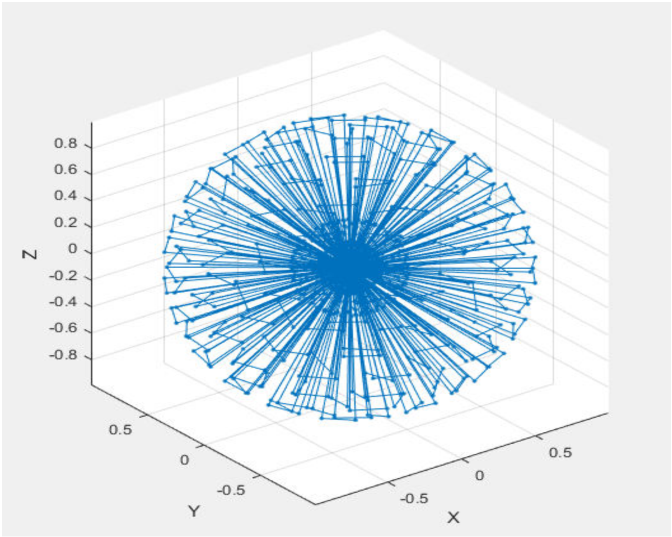

EPR Oxygen Imaging in an Animal

Proc. Natl. Acad. Sci. USA
Vol. 91, pp. 13047–13051, December 1994
Physiology

Oxymetry deep in tissues with low-frequency electron paramagnetic resonance

HOWARD J. HALPERN*, CHENG YU*†, MIROSLAV PERIC*‡, EUGENE BARTH*, DAVID J. GRDINA§, AND BEVERLY A. TEICHER¶

*Michael Reese/University of Chicago Center for Radiation Therapy and Department of Radiation and Cellular Oncology, University of Chicago, Chicago, IL 60637; §Division of Biolo ... ıstitute, Boston, MA 02115

Communicated by Cly

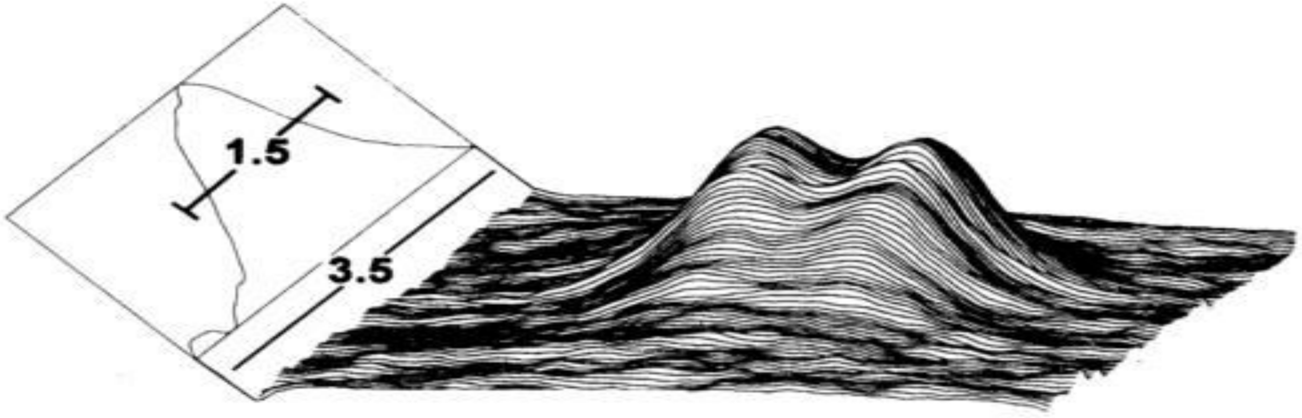

Spectral spatial (2D) image of a murine tumor

Continuous Wave Oxygen Image

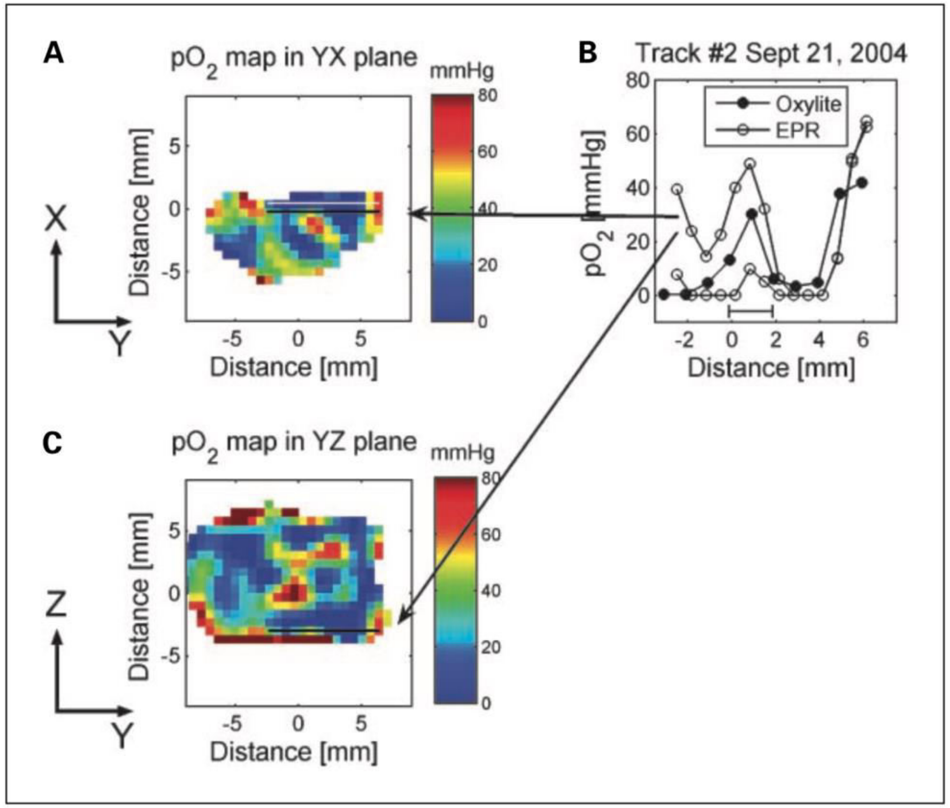

Correlation between Oxylite oxygen probe and EPR oxygen image

Dreher, M. R., M. Elas, K. Ichikawa, E. D. Barth, A. Chilkoti, G. M. Rosen, H. J. Halpern and M. Dewhirst (2004). Medical Physics **31**(10): 2755-2762.

pH imaging

6 ⇌ 6H+

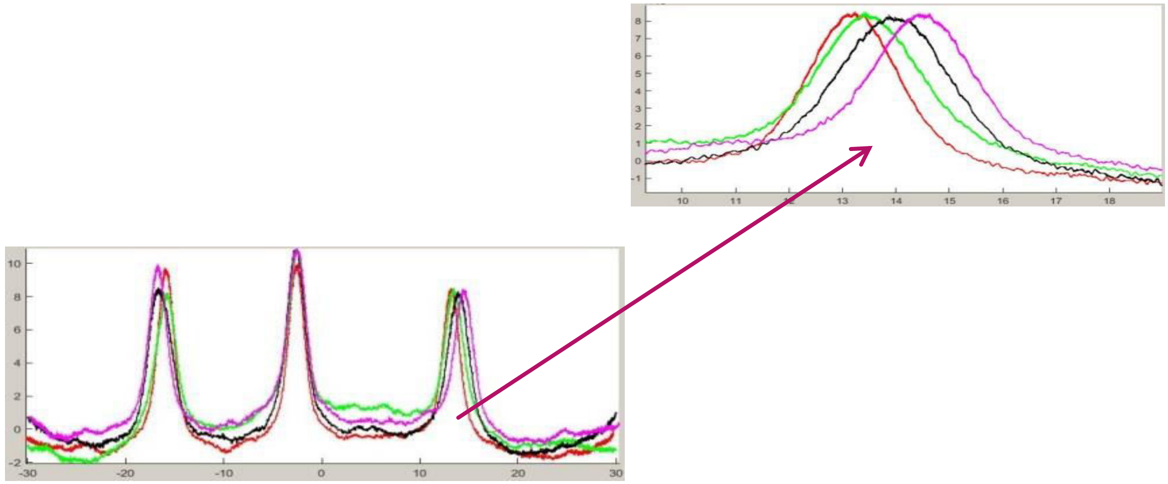

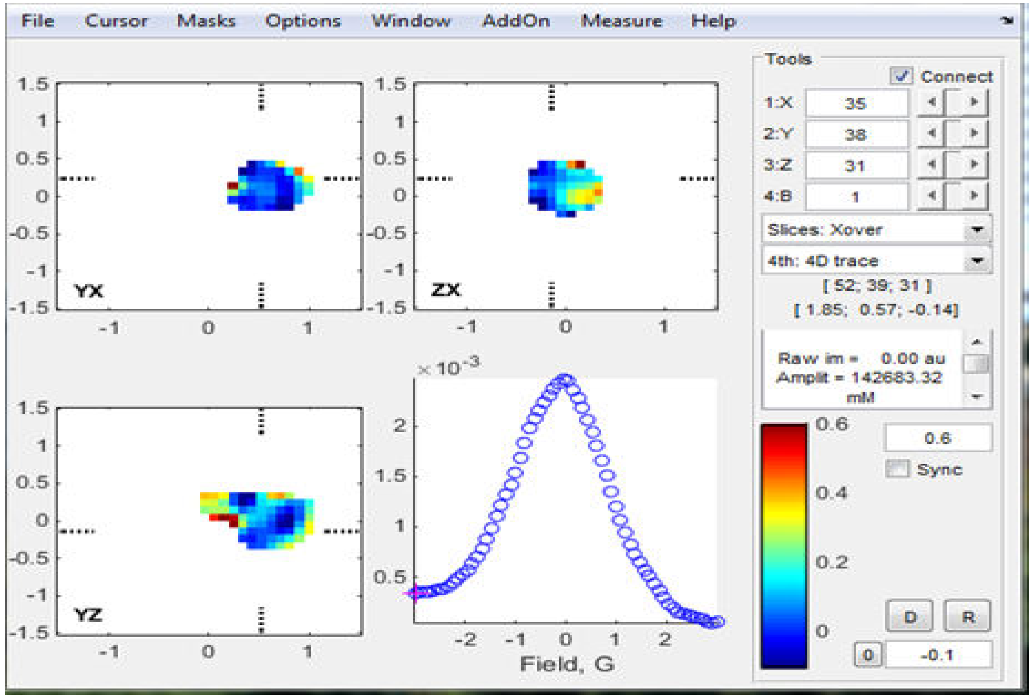

Li-Ion Batteries - Conduction Electron Paramagnetic Resonance Imaging

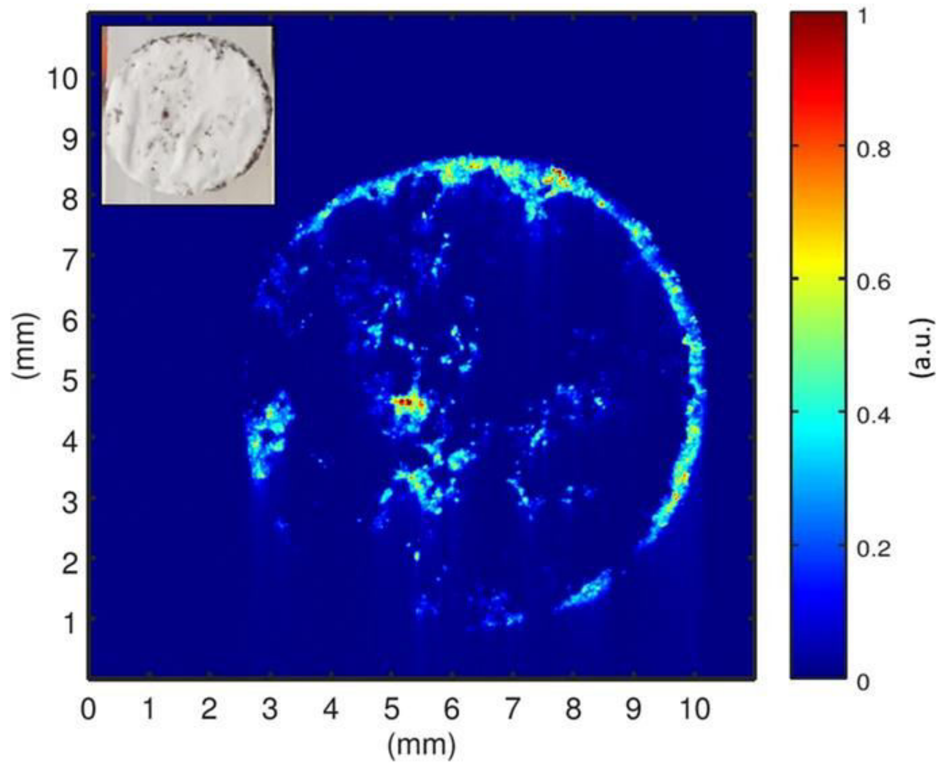

EPR image of lithium dendrites grown in a glass fiber separator with a diameter of 8 mm.

Niemöller, A., Jakes, P., Eichel, R. et al. EPR Imaging of Metallic Lithium and its Application to Dendrite Localisation in Battery Separators. Sci Rep 8, 14331 (2018)

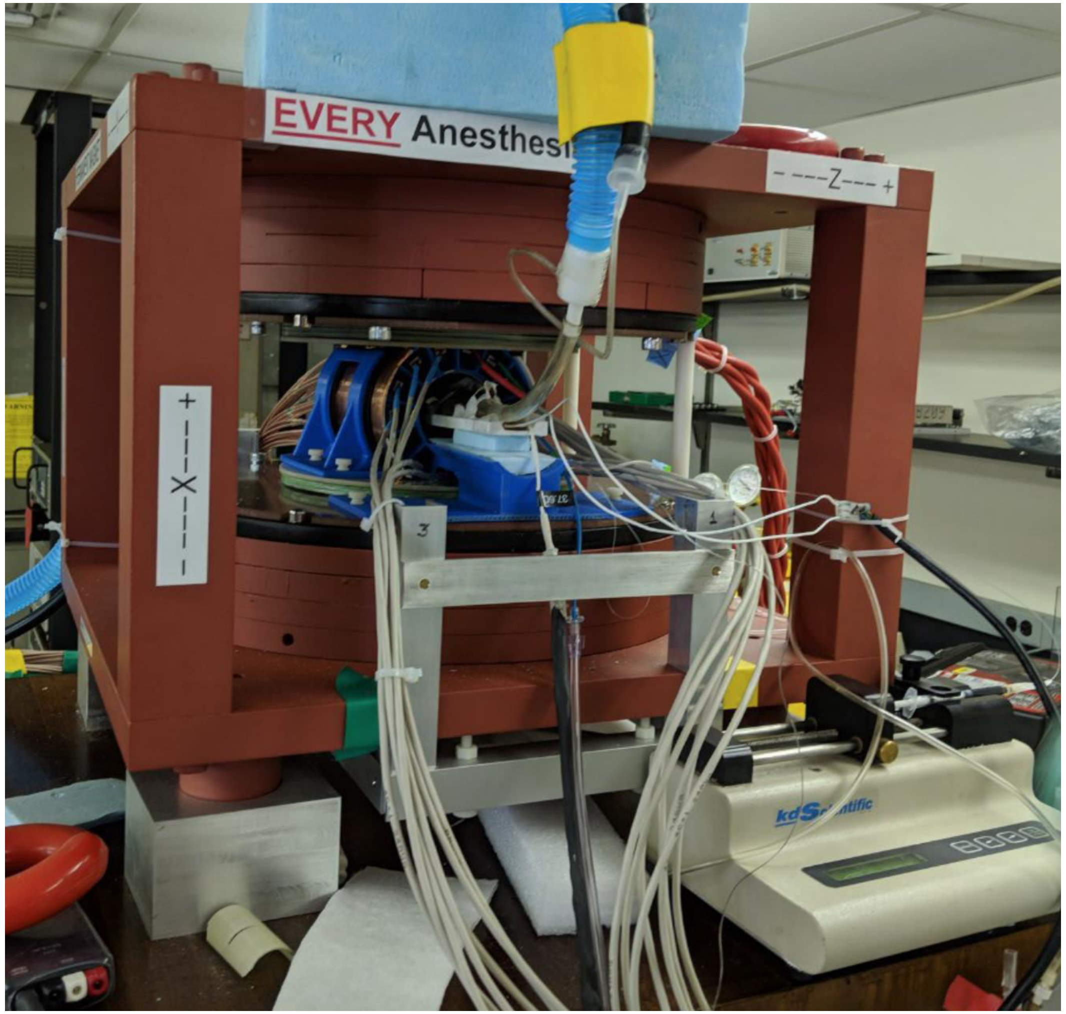

Challenges

Instrumentation Challenges

- Low concentration of spin-probe (low SNR)
- Fast relaxation (high power pulses)
- Scaling to large objects; limited penetration of RF into tissues at high frequencies
- Instrument size and weight
- Advanced image reconstruction algorithms
- Steep user learning curve
- Low tissue/sample contrast - other imaging method is required for spatial definition

EPROI needs complimentary imaging for spatial definition

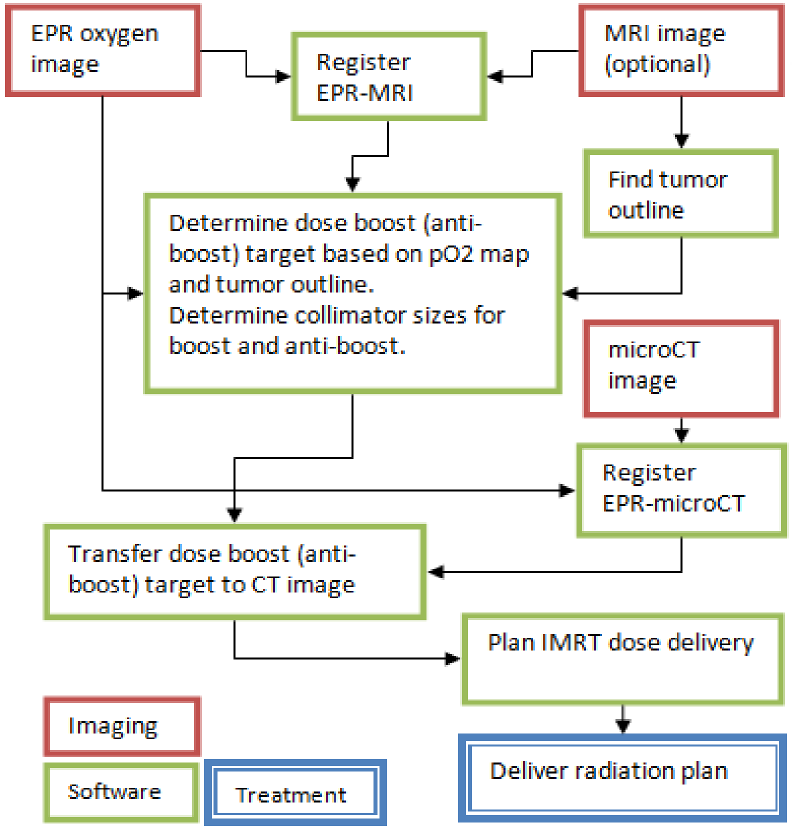

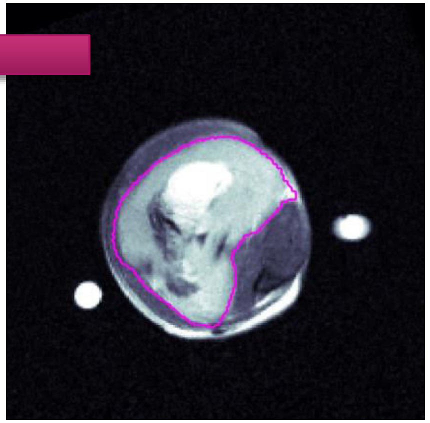

Anatomic MRI

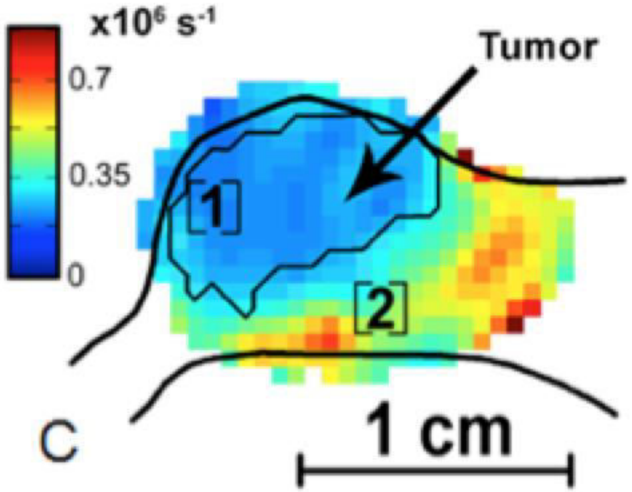

MATLAB Tools for Imaging

http://epri.uchicago.edu/

Temporary location: http://epr-it.specman4epr.com/

pvGUI – project manager
ArbuzGUI – image registration
ibGUI –image visualizer / statistics

Image processing, reconstruction, fitting, analysis, etc.

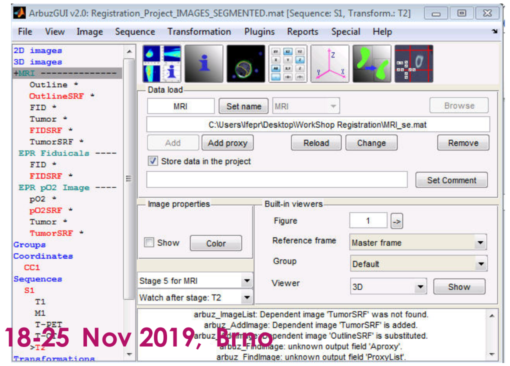

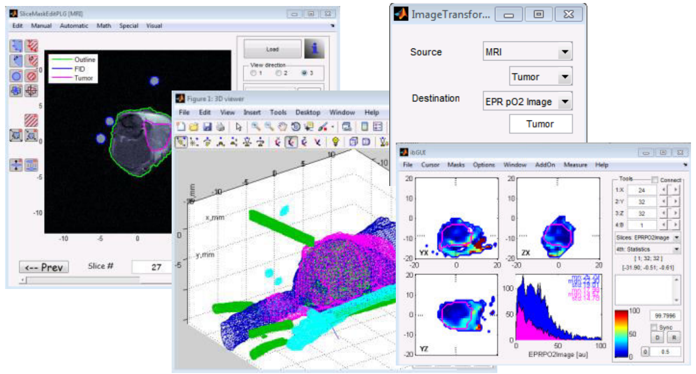

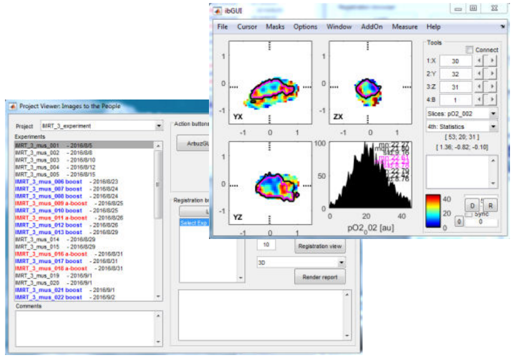

Literature

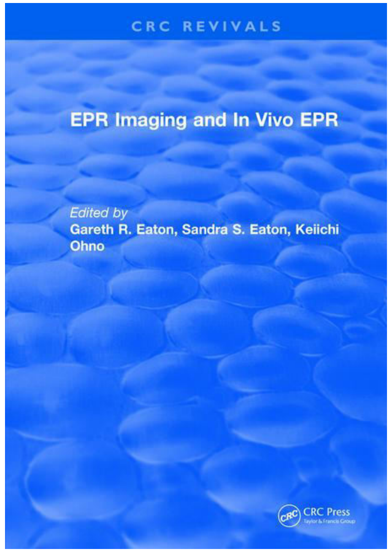

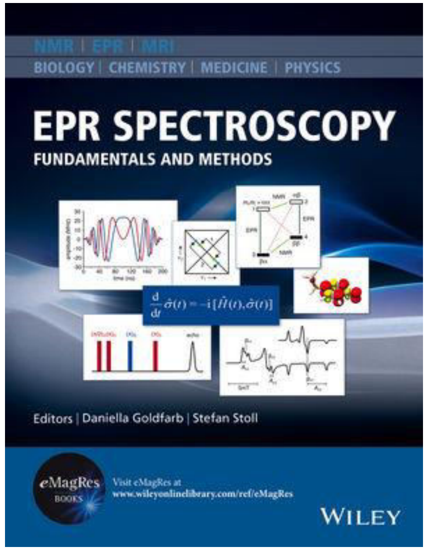

Eaton, G. R., S. S. Eaton and K. Ohno. EPR Imaging and in vivo EPR. Boca Raton FL, CRC Press (1991).

Epel, B. and H. Halpern. "EPR Imaging." in EPR Spectroscopy: Fundamentals and Methods, Eds. D. Goldfarb and S. Stoll, Wiley (2018) pp. 261-276